Stony Brook University

Microspheres composed of oxidized hyaluronan crosslinked gelatin as a drug delivery system for iNOS inhibitor

A Thesis Presented

by

Natalia Dmitrievna Ivanova

to

The Graduate School

in Partial fulfillment of the

Requirements

for the Degree of

Master of Science

in

Biomedical Engineering

Stony Brook University

December 2008

Stony Brook University

The Graduate School

Natalia Dmitrievna Ivanova

We, the thesis committee for the above candidate for the

Master of Science degree, hereby recommend

acceptance of this thesis

Weiliam Chen, Ph.D.
Thesis Advisor
Associate Professor, Department of Biomedical Engineering

Howard Fleit, Ph.D.
Committee Member, Outside Reader
Associate Professor, School of Medicine

This thesis is accepted by the Graduated School

Lawrence Martin
Dean of the Graduate School

Abstract of the Thesis

Microspheres composed of oxidized hyaluronan crosslinked gelatin as a drug delivery system for iNOS inhibitor

by

Natalia Dmitrievna Ivanova

Master of Science

in

Biomedical Engineering

Stony Brook University

2008

This project describes formulation and efficacy evaluation of oxidized hyaluronan crosslinked gelatin microspheres as a drug delivery system. Microspheres were prepared using a modified water-in-oil emulsion method, where formation of the microsphere core structure occurred without crosslinking reagents. Microsphere morphology analysis revealed rough surface in dry state and a highly porous structure upon swelling. Guanidinoethyl disulfide (GED) was used as a model drug; GED encapsulation and release were confirmed by HPLC. There was an inverse correlation between microsphere diameter and swelling ratio, and GED loading. Macrophages were used as a cell model to evaluate the efficacy of the drug delivery system. It was found that increased GED content had an inhibiting effect on cellular proliferation, density and viability. GED also inhibited release of nitric oxide (NO) and interleukin-1 beta (IL-1β) in activated macrophages. The effect of GED on tumor necrosis factor-alpha (TNF-α) was complex and will require further evaluations. The *in vivo*

efficacy and biocompatibility of microspheres were validated using mouse transcutaneous dermal wound model. Suppression of cell infiltration was observed in presence of GED.

TABLE OF CONTENTS

LIST OF ABBREVIATIONS

ATP	Adenosine triphosphate
DMEM	Dulbecco's Modified Eagle Medium
DNA	Deoxyribonucleic acid
FBS	Fetal bovine serum
GC	Glucocorticosteroids
GED	Guanidinoethyl disulfide
cGMP	Cyclic guanosine monophosphate
HA	Hyaluronic acid
H&E	Hematoxylin and eosin
IL-1β	Interleukin-1 beta
INF-γ	Interferon gamma
LPS	Lipopolysaccharide
NADPH	Nicotinamide adenine dinucleotide phosphate
NF-κB	Nuclear factor kappa-light-chain-enhancer of activated B cells
NO	Nitric oxide
eNOS	Endothelial nitric oxide synthase
iNOS	Inducible nitric oxide synthase
nNOS	Neuronal nitric oxide synthase
PBS	Phosphate buffer saline
STAT	Signal transducers and activator of transcription
TLR	Toll-like receptor
TNF-α	Tumor necrosis factor alpha

Constructs:

DDS	Drug delivery system
GOG	GED-loaded oHA/Gelatin hydrogel
OG	oHA/Gelatin hydrogel
oHA	Oxidized hyaluronan

LIST OF FIGURES AND TABLES

ACKNOWLEDGEMENTS

I would like to take this opportunity to thank Dr. Weiliam Chen, the principle investigator of this project, for his encouragement over the last two years. I am grateful for the opportunity he gave me to work in his lab and participate in this research. My work in Dr. Chen's lab has been funded by NIH grant DK068401.

I would like to express my deepest gratitude to Dr. Lihui Weng, a former post doctoral fellow in Dr. Chen's lab, for all her time and effort in teaching me new skills and concepts. I would not have been able to complete this work without her guidelines and support.

The text of this thesis in part is a reprint of the materials as it appears in: L. Weng, N. D. Ivanova, J. Zakhaleva, W. Chen. *In vitro* and *in vivo* suppression of cellular activity by guanidinoethyl disulfide released from hydrogel microspheres composed of partially oxidized hyaluronan and gelatin. *Biomaterials* **29**, 4149 (Nov, 2008). The co-authors listed in the publication directed and supervised the research that forms the basis for this thesis. A License was obtained from the publisher (Elsevier) for permission to use the content of the published material for this thesis.

I would like to thank Dr. Howard Fleit for his participation in the thesis committee, his time and effort. The meetings with Dr. Fleit in preparation of the thesis and his comments during the defense are greatly appreciated.

Dr. Julia Zakhaleva helped us during the animal studies, and I would like to thank her for the participation in our research.

I would like to thank all our lab members for their support over the last two years. Especially, I would like to acknowledge Christine Falabella, a Ph.D. candidate in Dr. Chen's lab, for her valuable advises.

In addition, I would like to acknowledge my professors from my graduate (SUNYSB-BME) and undergraduate (Carnegie Mellon, Chemistry) universities for the solid educational background they provided.

Finally, I would like to express my deepest gratitude to my family and friends, both in Russia and USA, for their constant support, encouragement and belief in me. I would not have been able to complete this work without it.

CHAPTER 1

HYPOTHESIS AND SPECIFIC AIMS

There has been an extensive interest in microsphere research in the last few decades. Microspheres can be formulated from synthetic or natural polymers; they serve as efficient vehicles for controlled release of drugs for achieving optimal efficacies. While synthetic materials are mechanically strong with more uniform physicochemical properties than their natural counterparts, their biocompatibilities are longstanding concerns. In contrast, natural polymers generally lack the mechanical strength and are less uniform in their physicochemical properties; they typically have less biocompatibility issues. Natural polymers can be modified to enhance their physicomechanical performance while retaining their biocompatibility.

Recently, hyaluronan-based microspheres, hydrogels and scaffolds have been devised, these vehicles showed good biocompatibility and promising results in tissue regeneration applications [Vercruysse et al. 1998; Liao et al. 2005]. Nonetheless, small molecule crosslinking reagents were generally deployed for their stabilization and the presence of residual reagents raised potential cytotoxicity issues. An approach free of small molecule crosslinker could circumvent these concerns.

Inducible nitric oxide synthase (iNOS) has been implicated in nitric oxide (NO) production in many inflammatory processes [Bosca et al. 2005]. Nitric oxide is an important messenger involved in regulation of inflammatory responses, vascular homeostasis and neurotransmission [Arzumanian et al. 2003]. However, excess NO could trigger acute and prolonged inflammatory responses, potentially detrimental to the

tissue [Coleman et al. 2001]. iNOS inhibition is a potential path for modulating many inflammatory processes.

In this project, we intend to demonstrate the feasibility of formulating hydrogel microspheres (or microgels) from naturally derived polymers utilizing an approach completely devoid of small molecule crosslinking reagents. Moreover, an iNOS specific inhibitor will be used as a model anti-inflammatory agent for encapsulation inside the microspheres to achieve prolonged action.

Our **hypothesis** is that the microsphere system composed of oxidized hyaluronan and gelatin is self-crosslinkable, biocompatible and biodegradable. The efficacy of the iNOS inhibitor, guanidinoethyl disulfide, in inhibiting activated macrophages could be prolonged by coupling it to the microspheres formulated. Accordingly, the Specific Aims are:

Specific aim 1: Formulation of self-crosslinkable microspheres composed of oxidized hyaluronan and gelatin as a carrier for an iNOS inhibitor, guanidinoethyl disulfide.

Specific aim 2: Efficacy evaluation of microspheres in an *in vitro* macrophage inflammatory model.

Specific aim 3: Evaluation of biocompatibility and efficacy *in vivo* of crosslinker-free microsphere system with incorporated iNOS inhibitor.

CHAPTER 2

INTRODUCTION

2.1 Wounds

Wound healing involves dynamic interactions of numerous cellular and molecular processes and can be categorized into three main stages: inflammation, tissue formation and remodeling. [Boateng at al. 2008].

2.1.1. Wound healing

The apparent goal of wound repair process is to re-establish the integrity of the damaged tissue. Hemorrhage typically occurs after injury, bacteria and antigens are eliminated from the wound during bleeding. In a blood-filled wound site, platelets are activated to form aggregates which, in turn, release clotting factors including fibrinogen, fibronectin and thrombospondin [Clark, 2001]. A newly formed fibrin clot blocks ruptured vessels, re-establishes hemostasis, and forms a provisional matrix setting that stage for cell infiltration [Clark, 2001].

Platelets entrapped inside wound space release chemoattractants and growth factors to draw leukocytes to the wound. Recruited neutrophils release enzymes and oxygen products to cleanse the wound area, however, overproduction of these substances could further damage the tissue [Clark, 1996]. Neutrophils are subsequently removed by macrophage or fibroblast phagocytosis. Monocytes migrate into the wound in response to monocyte-specific chemoattractants; in the wound monocytes undergo phenotypic changes and become macrophages capable of continuously secreting cytokines and

growth factors. [Fajiwara, 2005; Clark, 1996]. Macrophages play important roles critical for successful wound healing; macrophage-secreted cytokines cleanse the wound of bacteria and debris the secreted growth factors initiate tissue remodeling by attracting fibroblasts [Clark, 1996]. Therefore, macrophages provide an important link between inflammation and tissue regeneration stages.

Re-epithelization begins within a few hours post-injury [Clark, 2001]. Epithelial cells that migrate into the wound also undergo phenotypic changes, namely, dissolution of intercellular desmosomes and formation of peripheral actin filaments, these events collectively resulting in increased cell mobility and motility. As re-epithelization progresses, new basement matrix proteins are produced, epidermal cells revert to their native phenotype and attach to the basement matrix [Clark, 1996]. A defensive barrier is created during re-epithelization that protects the host against infection and water loss [Boateng et al. 2008].

Several days after injury, new capillaries, macrophages, fibroblasts and loose connective tissue, collectively known as granulation tissue, start to form [Boateng et al. 2008; Clark, 1996]. Macrophages and fibroblasts cooperatively interact during new tissue formation; cytokines released by macrophages stimulate angiogenesis and mediate fibroblast activity to create new extracellular matrix [Clark, 1996]. Newly formed blood vessels supply oxygen and nutrients, which in turn, support the migration and metabolism of more fibroblasts; the net outcome is an accumulation of large quantities of fibronectin, hyaluronic acid and collagen constituting the new extracellular matrix, while the fibrin matrix is being degraded [Clark, 2001]. The strength of the new tissue in the wound site

progressively increases with modifications of collagen by enzyme-mediated crosslinking. [Hackam, 2002].

2.1.2. Chronic wounds

Unlike normal wounds, chronic wounds do not heal beyond 12 weeks and often recur. This can happen in cases of multiple tissue insults or a physiological condition such as diabetes, infection and other pathological conditions [Boateng et al. 2008].

Diabetic patients are at greater risk of developing chronic ulcers. Due to hyperglycemia and decreased vascularization (hence, oxygenation), mediation of cellular activity is impaired [Harding et al. 2002]. In adipose tissues, elevated levels of inflammatory cells, specifically monocytes/macrophages (also attracted to the wound area during injury) have been observed. [Weisber et al. 2003]. Impairment of metabolism prolongs the inflammatory phase of wound healing sometimes becomes chronic [Harding et al. 2002]. Since macrophage activity is critical for transition of a wound bed from its inflammatory phase to re-epithelization, bioactive agents could be rationally devised to target inhibition of inflammation and induce wound healing in cases of chronic wounds.

2.2 Macrophages and inflammation

Macrophages are present in all organs and connective tissues, they have at least three major functions, namely, antigen presentation, phagocytosis and immunomodulation [Fujiwara et al. 2005]. Activation of macrophages is initiated by signals from T lymphocyte-derived cytokines (INF-γ, granulocyte-monocyte colony stimulating factor, and TNF-α), bacterial products (lipopolysaccharides, LPS), immune

complexes, chemical mediators and extracellular proteins such as fibronectin [Fujiwara et al. 2005]. Activation of macrophages triggers the release of transcription factor NF-κB that mediates expression of inflammatory cytokines, such as interleukin-1 (IL-1) and tumor necrosis factor alpha (TNF-α), and inducible nitric oxide synthase (iNOS) [Fujiwara et al. 2005]. Inflammatory cytokines continue to mediate iNOS expression leading to prolonged production of nitric oxide (NO) [Arzumanian et al. 2003].

2.2.1. iNOS/NO and inflammation

Nitric oxide is formed in cells by nitric oxide synthase (NOS) mediated conversion of L-arginine to L-citrulline [Hill et al. 1996]. There are three known isoforms of NOS that vary in amino acid sequence and their activity regulation mechanisms [Arzumanian et al. 2003]. Endothelial nitric oxide synthase (eNOS), located on the cell membrane, and neuronal nitric oxide synthase (nNOS), located in the cytosol, have similar mechanisms of action and are continuously expressed [Schwentker et al. 2002].

NOS exists in cells as a dimer with a reductase, a calmodulin-binding site and an oxygenase domain for each subunit. Ca^{2+}/calmodulin binding induces conformational changes in NOS enabling electron transport from NADPH on the reductase domain to the heme on the oxygenase domain for successful reaction between L-arginine and oxygen that results in NO production [Arzumanian et al. 2003]. Both eNOS and nNOS strongly depend on Ca^{2+} concentrations for their activation, and continuously produce small amounts of NO to maintain the basic level necessary for physiological processes.

Inducible form of nitric oxide synthase (iNOS) has calmodulin tightly bound and does not depend on calcium concentrations. However, iNOS is expressed only after excitation by bacterial toxin (LPS) or cytokines (IL-1, TNF-α, INF-γ) that activate tyrosine kinase receptors and Toll-like receptors (TLR) [Arzumanian et al. 2003]. Among proteins that react to tyrosine kinase receptor activation are signal transducers and activators transcription (STAT); they enter cell nucleus and induce iNOS expression [Arzumanian et al. 2003]. TLRs activate NF-κB transcription factor which also controls expression of iNOS as well as other pro-inflammatory cytokines [Coleman, 2001]; iNOS synthesis begins approximately two hours later and results in sustained production of large amounts of NO [Coleman, 2001; Arzumanian et al. 2003].

NO produced by NOS is a stable gas soluble in water and lipids. However, one electron turns NO into a reactive radical capable of penetrating cell membranes and become toxic when large amount is accumulated. One of the most important substrates of NO is cytosolic guanylyl cyclase responsible for the production of cyclic guanosine monophosphate (cGMP) leading to disconnection of actin-myosin links. Through this pathway NO mediates local blood circulation facilitating smooth muscle relaxation, and by cascade of events facilitates release of nerve-impulse in synapses [Arzumanian et al. 2003].

NO has the ability to replace oxygen during bio-energetic pathways in mitochondria, effect catalytic activity of metal-containing enzymes and block electron transport by binding to cytochrome heme group [Bosca et al. 2005; Arzumanian et al. 2003]. NO can also decrease mitochondrial inner membrane potential and induce swelling leading to mitochondria-dependent apoptosis; moreover, NO has the ability to

damage DNA by deaminization and block synthesis of glycolytic ATP [Bosca et al. 2005; Arzumanian et al. 2003]. Indirect effect of NO occurs through reaction with peroxide ions or oxygen to produce active forms of peroxynitrite ($ONOO^-$), inducing nitrosamine and oxidative stress [Coleman, 2001; Arzumanian et al. 2003].

Another important property of NO is mediation of cytokines, specifically IL-1. IL-1 is a highly inflammatory molecule; its systemic effects influence central nervous system, metabolism, hematology and vascular wall [Dinarello, 1997]. There is a strong correlation between the levels of NO and IL-1 observed in murine macrophages [Hill et al. 1996]. NO doesn't directly alter IL-1 expression, but it modifies its inhibitory factors (IL-1Ra or α2-microglobulin) by reducing their production [Hill et al. 1996]. The ability of NO to scavenge superoxide radicals by forming peroxynitrite also protects IL-1 from radical damage.

Similar effect has been shown for NO mediation of TNF-α – levels of cytokine-induced TNF-α increased with increase of NO, but decreased during LPS-stimulation [Eigler et al. 1993]. TNF-α is a principal mediator of acute inflammatory response; it acts by stimulating cells to produce chemokines, cytokines and acute phase proteins. In large quantities this cytokine can causes severe damage by entering the blood stream and acting as a hormone on liver, hypothalamus, and vascular system to cause severe metabolic disturbances [Abbas et al. 2007].

NO's capacity to inflict damages in microenvironments during inflammation and its role in partial mediation of inflammatory cytokines have made it and iNOS both attractive targets for pharmaceutical agents. Inhibition of iNOS/NO can potentially modulate chronic inflammatory responses.

2.3 Current anti-inflammatory treatments

A strong immune response is an important protective mechanism for an organism. However, this response could be destructive when inflammation reaches elevated levels and becomes persistent (allergies, autoimmune diseases). The choice of an appropriate drug is important in modulating chronic inflammations.

One of the most popular treatments currently used is glucocorticosteroids (GC). GCs inhibit NF-κB which is responsible for inflammatory cytokine expression, they also suppress NO through inhibition of NOS [Fujiwara et al. 2005]. Consequently, GCs suppress macrophage activation and induce apoptosis; they also decrease the number of circulating monocytes in the blood stream. GCs are also strongly suppressive to the immune system, however, their influence is systemic and may impair many normal organ and tissue functions.

Many agents with anti-inflammatory properties have recently been identified and they are capable of decreasing NO and inflammatory cytokine production; some examples are allylpyrocatecholin, cyanidin-2-O-β-glucoside and σ-3 fatty acid [Sarkar et al. 2008; Wang et al. 2008; Aldridge et al. 2008]. One of the agents with specificity for inducible form of nitric oxide synthase is guanidinoethyl disulfide (GED) [Szabo et al. 1997]. GED reacts with peroxynitrite and has protective effect against oxidative damage [Szabo et al. 1997]. Applications of GED *in vitro* and *in vivo* show that it could prevent β-cell destruction by peroxynitrite and development of Type I diabetes in NOD mice [Suarez-Pinzon et al. 2001; Mabley et al. 2004].

GED is typically given orally and this results in systemic side effects and a greatly decreased local efficacy. A polymeric drug carrier for localized GED delivery has not hitherto been attempted.

2.4 Polymers for drug delivery systems

Controlled drug delivery is one of the most intensely investigated areas of biomedical sciences. Drug delivery systems (DDS) have many advantages over systemic drug administration, these include site-specificity, optimal utilization, decreased toxicity, improved efficacy and convenience [Kumar et al. 2001]. DDS protects a drug from degradation, manage prolonged drug action and protects the microenvironment from irritation by the drug [Kumar et al. 2001]. Polymers utilized to formulate DDS should address several major issues including biocompatibility (both the polymer and its degradation by-products), biodegradability, and non-interference with the drug's efficacy. Microspheres are specific DDS with unique properties and broad applicability, their versatilities for formulations and modifications render them particularly attractive for biomedical applications. [Boateng et al. 2008].

Both synthetic and natural polymers have been used for microsphere formulations, with the latter being recognized as more biocompatible. Polymers most widely used include polylactide, polyglycolide, chitosan, dextran, etc. and their modified variants [Boateng et al. 2008]. Among natural polymers hyaluronic acid possesses special interest in DDS used for wound healing [Boateng et al. 2008; Yun et al. 2004].

2.4.1. Hyaluronan (HA)

Hyaluronan (HA) is a non-sulfated glycosaminoglycan composed of repeating units of D-glucuronic acid and N-acetyl-D-glucosamine. Biosynthesis of HA occurs in plasma membrane in the presence of HA synthase [Brown et al. 2005]. HA is a component of the extracellular matrix involved in many physiological processes such as water regulation, structural and space filling properties, lubrication, cell differentiation, and wound repair [Liao et al. 2005].

One of the most important properties of HA is water uptake, which induces hydration and formation of gel-like systems [Brown, 2005]. HA can be applied for direct treatment in osteoarthritis, surgery and wound healing (Healon®, Bionect®, Connettivina®), or used as a component in drug delivery for dermal, ophthalmic, nasal and pulmonary applications [Liao at al. 2005].

Native HA is highly soluble and degradable *in vivo* [Hornebeck, 2003]. Many crosslinking strategies and methods of modifications have been devised to prepare HA-based hydrogels, films and microspheres, with the overall goal of improving the physical parameters of HA while preserving its biocompatibility [Esposito et al. 2005]. Partial oxidation of HA opens up the ring structures of native HA, increases its elasticity and rendering it possible for crosslinking [Jia et al. 2004].

Previous work in our lab showed successful formulations of hydrogels prepared from oxidized HA and gelatin [Weng et al. 2008(a)]; this system was self-crosslinkable and completely devoid of small molecule crosslinking reagents which may have cytotoxic potential during hydrogel formation or after its degradation. This HA/Gelatin

hydrogel was biocompatible, non-cytotoxic and acquiescent to cell migration [Weng et al. 2008(a)].

2.4.2. Gelatin

Gelatin does not occur in nature, but is processed by thermal degradation of collagen isolated from mammalian skin and bones, or marine species. Approximately a third of amino acid composition consists of glycine; the polypeptide also contains a lot of proline and hydroxyproline [Ledward, 2000]. Proline-rich regions act as nucleation sites for junction zones, which are stabilized by inner chain hydrogen bonds at lower temperature [Ledward, 2000]. Once the temperature rises to 35-40 ^{o}C, those bonds break resulting in gel melting. Functional groups on amino acid side chains make gelatin a perfect component for crosslinked systems.

Gelatin is widely used in operating rooms as a surgical adjunct. It has been widely deployed in preparation of capsules, gels, sponges and microspheres [Ledward, 2000].

In this project, we propose to formulate a novel microsphere system composed of oxidized HA and gelatin for drug delivery. The system is self-crosslinkable and does not require any extraneous crosslinker. We further propose to use an iNOS inhibitor, guanidinoethyl disulfide, as a model drug, and believe that this delivery system will provide and enhance the localization of the drug and sustain its efficacy.

CHAPTER 3

SYNTHESIS AND CHARACTERIZATION OF MICROSPHERES

Specific aim 1: Formulation of self-crosslinkable microspheres composed of oxidized hyaluronan and gelatin as a carrier for an iNOS inhibitor, guanidinoethyl disulfide.

Experiments and analyses described in this chapter were done in collaboration with Dr. Lihui Weng, a former Post-doctoral Fellow in Weiliam Chen's lab. Both Natalia Ivanova and Lihui Weng participated in all of the experiments, and the contribution was equal. The results presented in this chapter were published: L. Weng, N. D. Ivanova, J. Zakhaleva, W. Chen. *In vitro* and *in vivo* suppression of cellular activity by guanidinoethyl disulfide released from hydrogel microspheres composed of partially oxidized hyaluronan and gelatin. *Biomaterials* **29**, 4149 (Nov, 2008).

3.1 Materials and Methods

3.1.1. Materials

Gelatin (Bloom 300, Type A, M_w 100,000) was purchased from Sigma-Aldrich (St. Louis, MO, USA). Guanidinoethyl disulfide (GED) was purchased from Inotek (Beverly, MA, USA). Oxidized hyaluronan (oHA) was prepared using a previously described method [Weng et al. 2008(a)]. All other chemicals were of reagent grade and deionized water was used.

3.1.2. Formulation of oHA/Gelatin microsphere

The microspheres were prepared using a modified water-in-oil emulsion method. For a typical preparation, briefly, a 2% (w/v) aqueous gelatin solution (5 ml) was mixed with an equal amount of a 2% (w/v) aqueous oHA at 37^{o}C. The mixture was added to pre-heated soya oil (60 ml) containing pre-dissolved Span 80 (1 ml), maintained at 50^{o}C with a water bath, while under agitation by a mechanical stirrer at a speed 1,100 rpm to form an emulsion. After 24 hours, the microspheres formed were recovered by precipitation with 60 ml of cold isopropanol. The oil phase was removed after 5 minutes of additional stirring and 10 minutes of centrifugation at a speed of 9,000 rpm. The microspheres were then washed three times with 30 ml of a 1:1 mixture of acetone/isopropanol and air dried at room temperature.

3.1.3. GED incorporation

Aqueous GED of concentrations 0.2, 1 and 2% (w/v) were, respectively, incorporated into the gelatin/oHA mixture before emulsion formation by adding 1 mL of preheated GED solution (at 37^{o}C). Microspheres were prepared according to the method described in section 3.1.2.

3.1.4. Morphological and size analysis of the microspheres

Analyses of dried and lyophilized (i.e., after hydration and fully swollen) microspheres were performed by scanning electron microscopy (SEM) (SFEG Leo 1550, AMO GmbH, Aachen, Germany). Size distributions were evaluated under light

microscopy (Olympus, IX-71, Tokyo, Japan) and the images were digitized by QCapture 5 imaging software (Surrey, Canada).

3.1.5. Microsphere GED content

The amount of encapsulated GED was determined by extracting 2 mg of GED-loaded microspheres in 5 mL of 0.01M HCl and agitating at 37°C for 3 days. The amount of GED recovered was analyzed by HPLC (column: Supercoil LC-18DB, 250 × 4.6 mm; mobile phase: 3% acetonitrile in 20 mM KH_2PO_4, pH 3.0; flow rate: 0.8 mL/min; detection: UV 245 nm).

3.1.6. In vitro GED release from microspheres

GED-loaded microspheres with GED concentrations of 0.2, 1 and 2% (n = 3) were dispersed in 1 mL of pH 7.4 PBS, incubated at 37°C under constant agitation. Aliquots of releasates (100 μL) were collected after centrifugation of samples and replenished with equal amounts of PBS. Sample collection time-points were 0.5, 1, 3, 5, 7, 10, 24, 72, 120 and 168 hours; the GED concentrations were determined by HPLC (column: Supercoil LC-18DB, 250 × 4.6 mm; mobile phase: 3% acetonitrile in 20 mM KH_2PO_4, pH 3.0; flow rate: 0.8 mL/min; detection: UV 245 nm).

3.1.7. Microsphere swelling

Microspheres were place in PBS (pH 7.4) at 37°C. Images were captured under a microscope at: 1, 3, 5, 10, 15, 30, 45 s; and 1, 2, 3, 5, 7, 10, 15, 20 and 30 minutes. The

swelling ratio (q) was calculated using Equation 1 with the assumption of spherical particle geometry.

$$q = V_{wet}/V_{dry} \quad \text{(Eq. 1)}$$

where V_{wet} is the volume of a swollen microsphere at given time, and V_{dry} is the volume of the dried microsphere at time 0.

3.1.8. Statistical analysis

All experiments were preformed with at least three replicates. Results were expressed as mean ± standard error. One-way ANOVA test (p<0.05) was done to determine the presence of difference between the sample means in the tested population. Further, Post-hoc Tukey's test with significance level set at 0.05 was done to determine which samples were significantly different from each other.

3.2 Results and Discussion

3.2.1. Formulation of Microspheres

The microspheres were formulated from oxidized hyaluronan (oHA) and gelatin using a water-in-oil emulsion method. Oxidation of HA produced oHA with oxidation degree of 44.7%, as described previously [Weng et al. 2008(a)]. Oxidation of HA opened ring structures and created multiple aldehyde groups capable of reacting with amino groups on gelatin thus, forming a 3-D hydrogel structure through Schiff base formation [Weng et al. 2008(a)]. This reaction occurred in aqueous phase, without any small molecule crosslinking reagents; the reaction mechanism was revealed previously schematically presented in Figure 1 [Weng et al. 2008(a)]; the amino groups on GED

could also participate in reaction with oHA. However, formation of those bonds is partially inhibited by the presence of azane-bicarbonate in close proximity to amines.

GED was introduced into the structure at the initial stage of the formulation process. oHA/Gelatin microspheres were prepared with 0.2, 1 and 2 % GED aqueous solutions. The encapsulation efficiency of the system was summarized in Table 1 and it ranged from 37 to 76 %, suggesting that the microspheres' GED contents could be modulated.

3.2.2. Morphological and Size Analyses of Microspheres

The results of microsphere morphological analyses were presented in Figure 2. The SEM images included plain (oHA/Gelatin) microspheres (Fig. 2 A, C) and 1% GED-loaded microspheres (Fig. 2 B, D) in their dried and hydrated/swollen (after lyophilization) state. The microspheres in their dried state showed a coarse surface with small pores. It was also noticed that the diameters of microspheres with 1% GED loading were generally smaller than their counterparts without GED. The swollen lyophilized microspheres showed morphological changes during swelling – highly porous with increased pore sizes. The elliptical shape of the microspheres was most likely the result of the drying process.

The size distributions of four microsphere formulations (0, 0.2, 1 and 2 % GED loadings, respectively) were depicted in Figure 3. The mean sizes of microspheres containing 0, 0.2, 1 and 2 % GED were 91.6 ± 18.8 (Fig. 3A), 86.3 ± 19.7 (Fig. 3B), 56.4 ± 9.4 (Fig. 3C), and 31.4 ± 8.7 μm (Fig. 3D), respectively, and the results were summarized in Table 1.

There was an inverse correlation between the GED concentration and the microsphere diameter as well as the spread of the diameter distribution – while the GED concentration increased from 0 to 2%, the diameter decreased from 91 to 31 μm and the spread of the distribution became narrower. The increase in GED concentration could decrease the viscosity of the liquid in aqueous phase during microsphere formulation, which would result in formation of smaller emulsion droplets and consequently smaller microspheres. Moreover, the abundance of amino groups on GED could react with the aldehyde groups on oHA thus, further crosslinking the internal structures and thus, further the stability of the microspheres formed (Figure 1).

3.2.3. Microsphere Drug Content and Release in vitro

The HPLC eluent profiles were presented in Figure 4. The peak around 13 minutes in the GED standard profile was also present in the microsphere release sample, which supported the hypothesis of successful GED encapsulation and release. Multiple peaks appeared along the profile were indicative of microsphere degradation. GED encapsulation yield (%) was summarized in Table 1.

In vitro GED release kinetics was observed over the course of 1 week and the results were summarized in Figure 5. During the first 7 hours, a burst release of GED was observed in each sample (0.2, 1 and 2 % GED content). Comparable kinetics were previously reported in similar systems prepared by physical entrapment [Cortesi et al. 1999]. The burst phase was indicative of the rapid detachment of free GED physically associated with the microsphere surface that was not removed during washing. After the burst phase, a continuous slow release was observed for 1 week. While this system was

able to prolong GED's efficacy, it was less able to produce a truly controlled release profiles. Recovery of GED was proportional to the initial amounts of GED incorporated into microspheres (i.e., 4, 10 and 30 μg/mg microsphere for 0.2, 1 and 2 % GED-loaded microspheres, respectively).

3.2.4. Microsphere swelling

Images of swollen microspheres and swelling kinetics were presented in Figure 6. The swelling equilibrium was reached rapidly (500 s) and the microsphere GED content played an important role in the swelling kinetics. The swelling ratio (q) increased from 6.02 to 19.82 with the increase of initial GED content from 0 to 2 %. Due to its structure GED could interfere with the interaction between the amino groups of gelatin and aldehyde groups of oHA, leading to a decrease of crosslinking density and thereby, greater degree of swelling.

Figure 1. Schematic representation of microspheres core formation from oxidized hyalronan (oHA), gelatin and guanidinoethyl disulfide (GED).

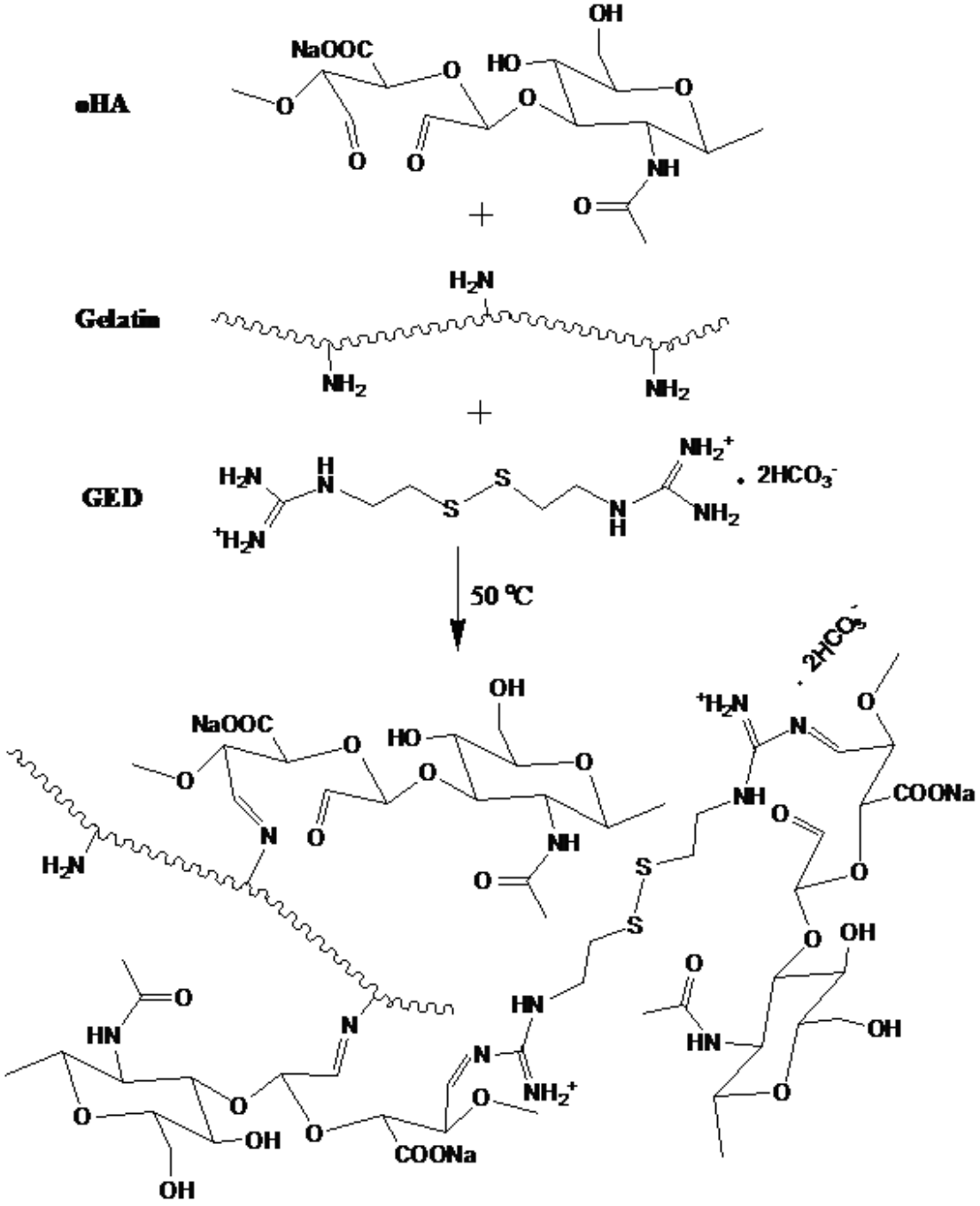

Table 1[1]. Particle size distribution of plain oHA/gelatin microspheres and GED-loaded microspheres.

Microsphere composition	Mean diameter (μm) ± SD	GED encapsulation yield (%)
OHA/Gelatin	91.56±18.76	--
OHA/Gelatin/0.2%GED	86.28±19.69	76.64
OHA/Gelatin/1%GED	56.39±9.43	70.98
OHA/Gelatin/2% GED	31.39±8.67	37.4

[1] Table was adapted from Weng et al. 2008(b).

Figure 2[2]. Scanning electron micrographs of plain (A, C) and 1% GED loaded (B, D) oHA/gelatin microspheres. (A) and (B): original dry state; (C) and (D): full hydrated/swollen and lyophilized.

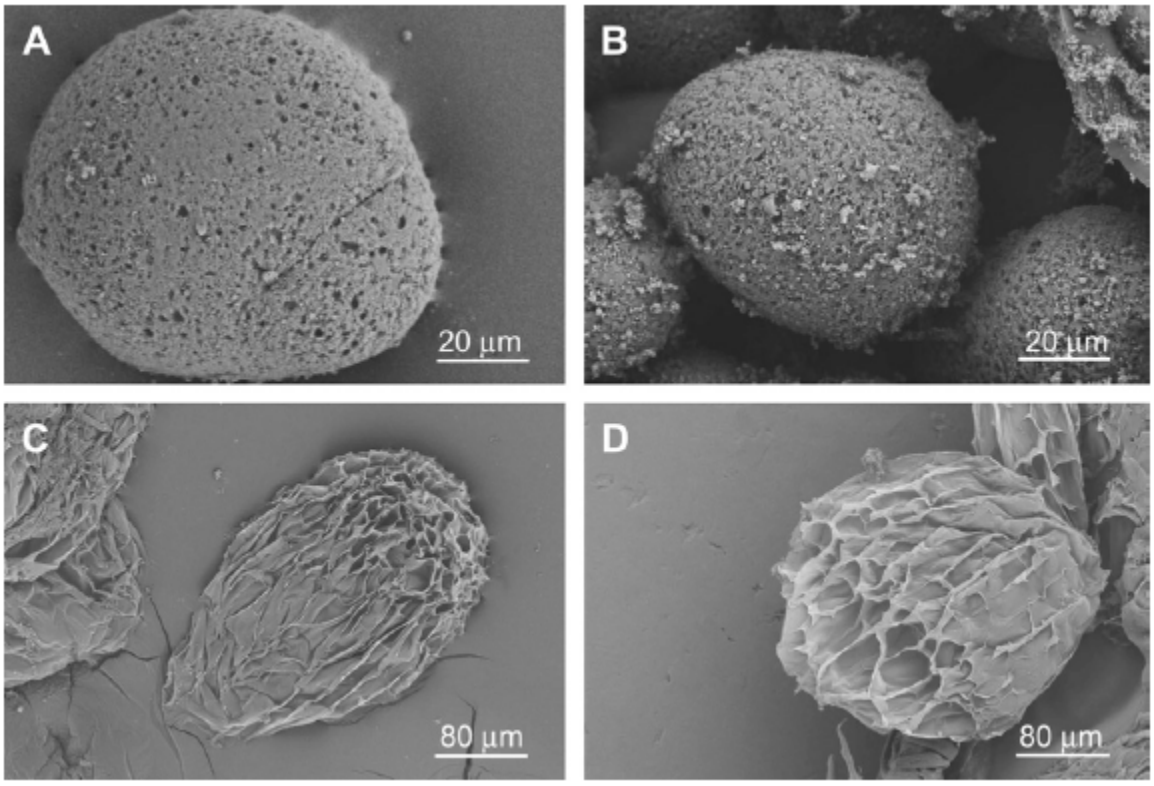

[2] Image was adapted from Weng et al. 2008(b).

Figure 3[3]. Size distribution plots of oHA/gelatin microspheres: plain (A), 0.2 % (B), 1 % (C) and 2 % (D) GED content.

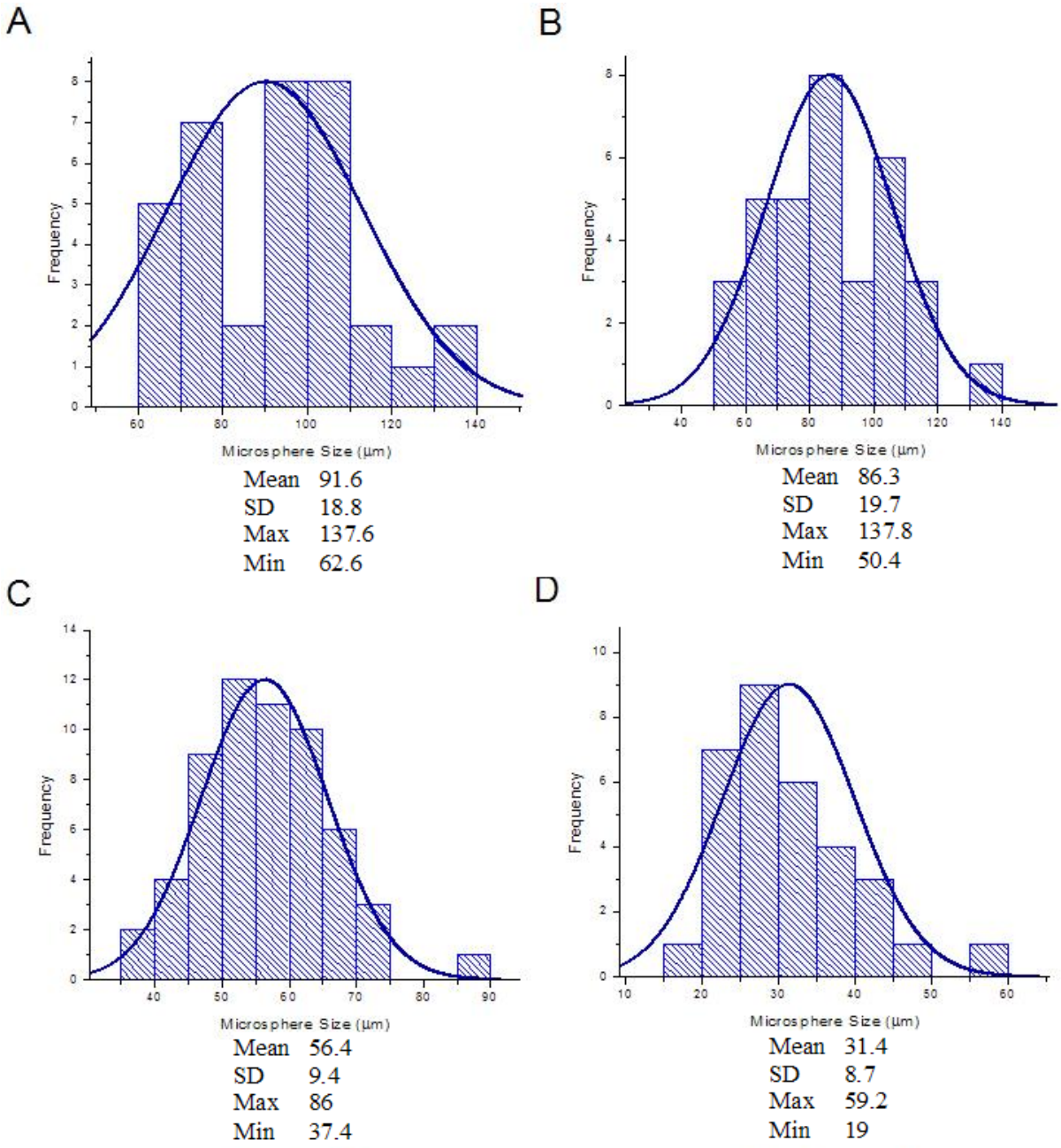

[3] Modified image was adopted from Weng et al. 2008(b).

Figure 4[4]. HPLC elution curve of a sample from release test of 1% GED-leaded oHA/Gelatin microspheres (A) and a standard GED solution (B).

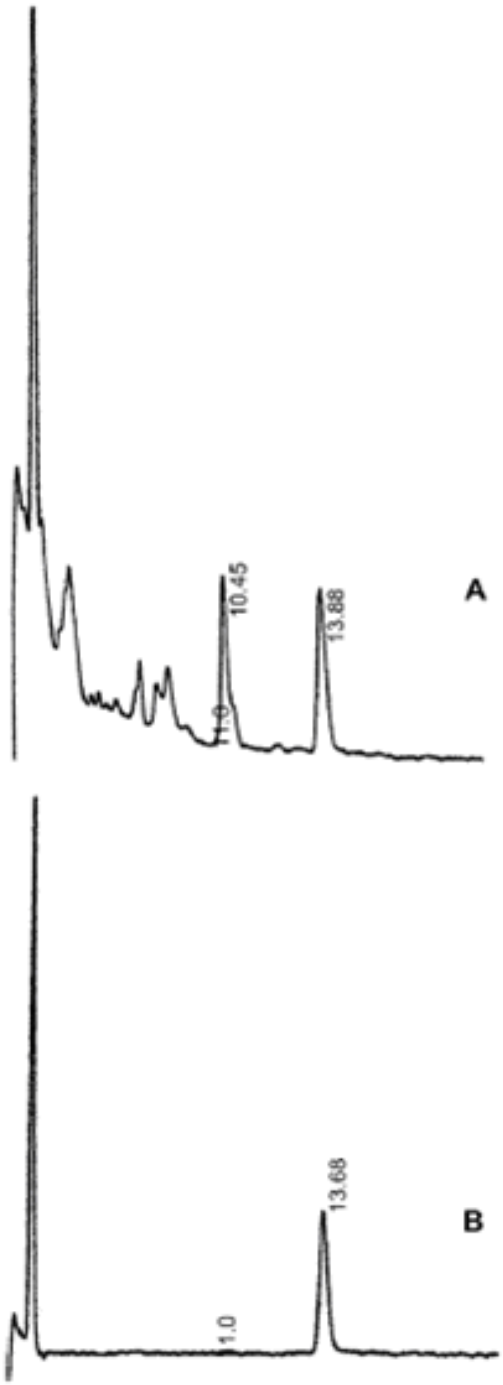

[4] Image adopted from Weng et al. 2008(b).

[5]Figure 5. GED release profiles of oHA/Gelatin microspheres with 0.2, 1 and 2% GED content.

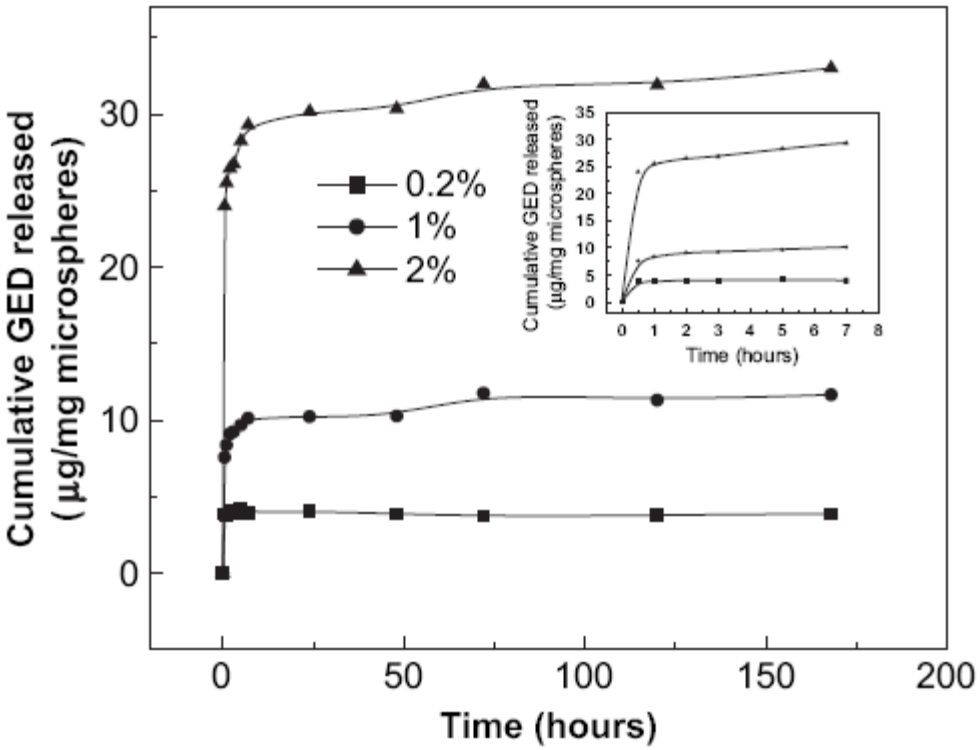

[5] Image was adopted from Weng et al. 2008(b).

Figure 6[6]. Swelling of oHA/Gelatin microspheres. (A) Photograph of swollen GED-loaded microspheres. (B) The effect of GED content on the microspheres swelling dynamic.

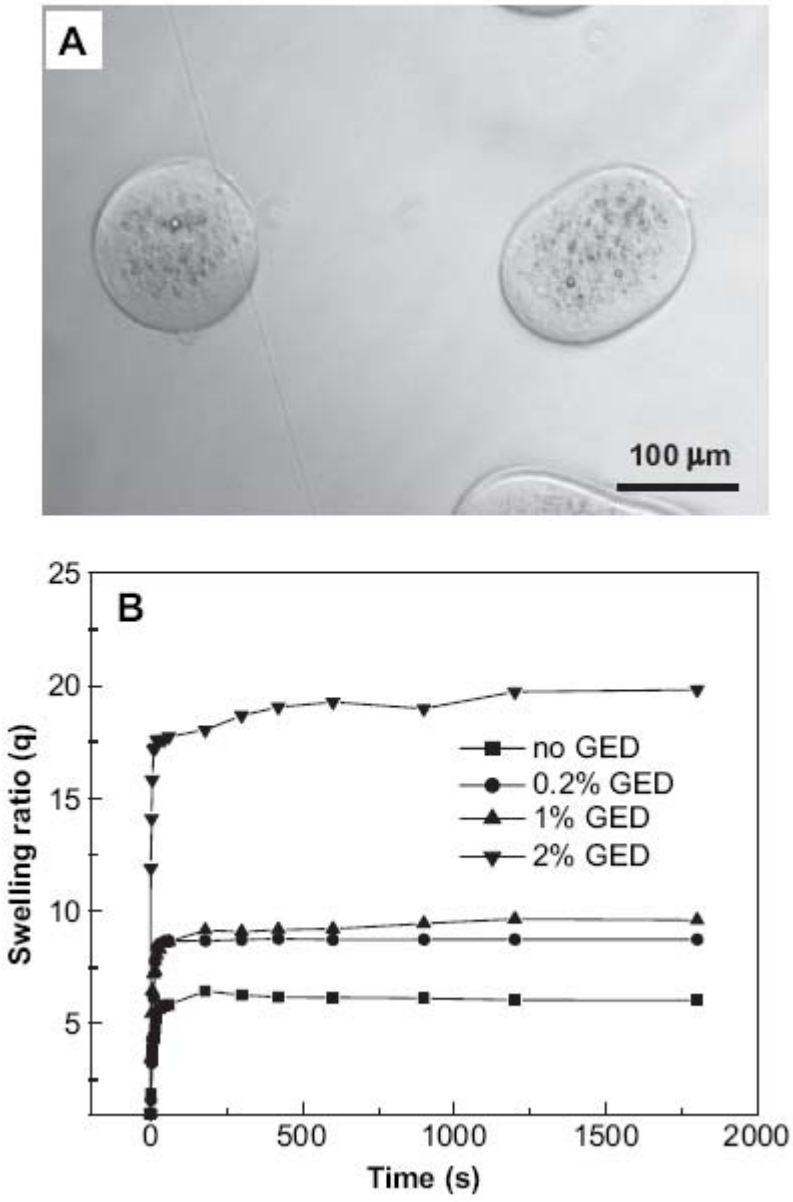

[6] Image was adopted from Weng et al. 2008(b).

CHAPTER 4

IN VITRO EFFECT OF THE INOS INHIBITOR RELEASED FROM MICROSPHERE SYSTEM

Specific aim 2: Efficacy evaluation of microspheres in an *in vitro* macrophage inflammatory model.

Experiments and analysis described in this chapter were completed by Natalia Ivanova.

4.1 Materials and Methods

4.1.1. Materials

Macrophages (murine, RAW264.7, ATCC, Manassas, VA, USA) were grown in high glucose DMEM (Gibco, Grand Island, NY, USA) supplemented with 10% FBS (Hyclone, Logan, UT, USA) and 1% Pen/Strep (Gibco, Grand Island, NY, USA) at 37^{o}C in a humidified atmosphere of 5% CO_2. Cell viability was determined using MTS kit (Promega BioSciences, San Luis Obispo, CA USA). Nitric oxide release from macrophages was detected using Griess Reagent kits (Molecular Probes, Eugene, OR, USA). The amounts of cytokines released (IL-1β and TNF-α) were determined with ELISA kits (Molecular Probes, Eugene, OR, USA). All other chemicals were of reagent grade and deionized water was used.

4.1.2. Hydrogel film formulation

All experiments involving cell cultures were done using a direct-contact mode, where cells were seeded onto 0.5 mm thick hydrogel films containing GED-loaded microspheres. To prepare the hydrogels, GED-loaded microspheres were dispersed in oHA/Gelatin solution following a previously established procedure [Weng et al. 2008(a); Weng et al. 2008(b)]. Respectively, microspheres of 0.2%, 1% and 2% GED-loadings, were dispersed in solutions composed of 20% (w/v) oHA/ 20% (w/v) Gelatin (4:6 ratio) with 0.1M borax. The mixtures were incubated at 37^{o}C for 24 hours followed by one additional week incubation at 4^{o}C.

4.1.3. Cell proliferation and viability

To test cell proliferation in the presence of GED, cells were seeded on hydrogel films prepared as described in section *4.1.2*. Briefly, 5×10^4 macrophages were seeded per well (24-well plate) (n=3) without hydrogel (as the control group), on oHA/Gelatin hydrogel films (OG), on oHA/Gelatin hydrogels containing 0.2, 1 or 2% GED-loaded microspheres (coded as 0.2% GOG, 1% GOG and 2% GOG, respectively). The media were changed daily and cell-laden hydrogels were observed to determine cell morphology and density on days 3, 6, 10 and 14, respectively, under light microscopy (Nikon Diaphot, Tokyo, Japan); images were digitally captured (Nikon D200, Tokyo, Japan). Cell densities were presented as the average number of cells per 100 μm^2 ± S.E.M.

Cell viability was, respectively, determined using MTS assay on days 3, 6, 10 and 14 (n=3). Following manufacturer provided protocol, briefly, MTS solution was added to

each well (5 µl/100 µL media) and the mixture was incubated in dark for 1 hour at 37^{o}C. This was followed by removal of 200 µl of supernatant from each well and the absorbance was determined at 490 nm by a microplate reader (Infinite M200, Tecan US, Research Triangle Park, NC, USA). The results were presented as average absorbance ± S.E.M.

4.1.4. NO release

The nitrite contents of cell culture media were determined by Griess assay following manufacturer provided protocols. Macrophages (5×10^5) were seeded following the protocol described above (*4.1.2.* and *4.1.3.*, n=6 for each). After 3 h incubation half of samples were treated with LPS (2 µg/ml); the nitrite contents were determined 24 h later. Briefly, 150 µL of sample were mixed with 130 µL of deionized water and with 20 µL of Griess reagent (0.1% NED in water and 1% sulfanilic acid in 5% phosphoric acid). The mixture was incubated in dark at room temperature for 30 minutes and absorbance was determined at 548 nm by a microplate reader (Infinite M200. Tecan US, Research Triangle Park, NC, USA). The resulting nitrite concentrations in samples were determined from a previously prepared standard plot and presented as average ± S.E.M.

4.1.5. Cytokine (IL-1β, TNF-α) release (ELISA)

The experiment was setup as described in section *4.1.4*. After 24 h of LPS treatment, cell-free media were collected and stored at -80^{o}C until use. The cytokine concentration was determined using sandwich Enzyme Linked-Immuno-Sorbent Assay

(ELISA) kits, specific for mouse TNF-α and mouse IL-1β, respectively. Sample absorbances were determined at 450 nm by a microplate reader (Infinite M200, Tecan US, Research Triangle Park, NC, USA). Standards for each protein were prepared according to manufacturer provided manuals (0-1,000 pg/ml). Protein levels in the samples were calculated from a previously prepared standard curves and the results were presented as average ± S.E.M.

4.1.6. Statistical analysis

All experiments were preformed with at least three replicates. Results were expressed as mean ± standard error. One-way ANOVA test ($p<0.05$) was done to determine the presence of difference between the sample means in the tested population. Further, Post-hoc Tukey's test with significance level set at 0.05 was done to determine which samples were significantly different from each other.

4.2. Results and Discussion

Macrophages are important cells in mediation of inflammatory processes. NO and cytokine production by macrophages rises sharply in response to inflammatory stimuli. Modulation of macrophage activity can potentially influence the severity of the inflammatory response. Therefore, macrophage cell culture was selected for efficacy validation of GED-loaded microspheres *in vitro*.

4.2.1. Cell proliferation, density and viability

Cell proliferation, density and viability were determined at 3, 6, 10 and 14 days, respectively. Figure 7 illustrated cell morphology and distribution at days 3 and 14 for the control group (A, B); macrophages in OG group (C, D), in 0.2% GOG group (E, F), in 1% GOG group (G, H), and in 2% GOG group (I, J).

Cell density, as number of cells per 100 μm^2, was presented in Figure 8 (A). Cell number decreased with increase of GED content during the course of the study. Different patterns of cell proliferation at various time points were also revealed. Cells in the control group spread uniformly and reached full confluence by day 10. In contrast, cells in the OG group proliferated less uniformly; specifically, cells seeded on top of the hydrogel film developed into large colonies and grew on each other forming layers until day 6. Later cells started to spread over the surface of the hydrogel but still didn't reach full confluence by day 14. Observations of cell morphology showed that more cells appeared to be activated compared to the control group (Figure 7 (D)).

Cells in 0.2% GOG group had a proliferation pattern comparable to those in the OG group. The colonies were noticeably smaller and the cells tended to grow within them forming layers. By day 10 cells started to proliferate over the hydrogel surface. However, by day 14 the presence of scattered pockets of unoccupied areas, mostly around GED-loaded microspheres, was evident. The cell density of 0.2% GOG group as shown in Figure 8 (A) illustrated a progression of cell growth with time, but the cell density at day 14 was significantly lower ($p<0.05$) than its counterpart in the OG group due to the presence of GED.

Macrophages in 1% GOG group showed different growth patterns than macrophages in OG and 0.2% GOG groups. Overall, the sizes of cell clusters formed by day 3 in 1% GOG groups were smaller than those formed in the 0.2% GOG group, and contained usually no more than 5 cells each. Figure 7 (H) clearly illustrated that cells of the 1% GOG group continued growing in clusters by day 14 without proliferating on the surface of the hydrogel film. Increase in GED content in 1% GOG group compared to 0.2% GOG group was manifested by fewer activated cells present and larger areas not occupied by cells. Figure 8 (A) showed a moderate increase in cell density from day 3 to day 6, with its magnitude markedly elevated from day 10 to day 14. This was most likely related to the GED release kinetics discussed in Chapter 3. It should be noted that daily change in cell culture media precluded effective accumulation of GED released, thereby, leading to an increase in cell growth.

The proliferation patterns of cells seeded on 2% GOG were comparable to those of cells in 1% GOG group. As depicted in Figure 7 (I) and 8 (A), the inhibition effect was prominently shown by day 3 as the culture plate was sparsely populated, primarily by isolated cells instead of cell clusters. A very modest increase in cell density was observed by day 6; the magnitudes of cell density increase were more prominent by day 10 and 14. In fact, the cell densities of 2% GOG and 1% GOG groups were comparable, most likely due to the loading efficiencies of 1 and 2% GED microspheres. As summarized in Table 1, in Chapter 3, the loading efficiencies were 70.98% and 37.4% for 1% and 2% GED microspheres, respectively, resulting in approximately equal total amounts of encapsulated GED. Sufficient amount of GED was released during the initial stage of the study to achieve a prominent suppression of cell proliferation; due to the

subsequent moderation of GED release, this suppression effect was reversed with progression of time and cell growth eventually resumed.

In parallel, cell viability was observed at every time point (3, 6, 10 and 14 days) and the results were summarized in Figure 8 (B), with its pattern mirroring Figure 8 (A). However, in the study, the culture media were changed daily leading to the inevitable removal of dead cells, it could thus be inferred that GED, at a proper concentration range, suppressed cell proliferation instead of killing the cells and this effect lingered on. This raised the issue of whether GED was implicated in mediating cell apoptosis, which could be a topic for future investigation.

4.2.2. NO release

Sample nitrite concentrations, as surrogate endpoint of NO activities, were determined and the results (average ± S.E.M) were presented in Figure 9. After 24 hours, the nitrite content of the control group at its resting state was 4.72 ± 1.21 μM, this was dramatically increased to 32.95 ± 1.4 μM 24 hours after exposure to LPS (2 μg/ml). The media nitrite content in OG group was 20.69 ± 2.86 μM after incubating for 24 hours at resting state, and 21.93 ± 0.86 μM 24 hours after LPS stimulation, suggesting that macrophages were activated even without LPS stimulation; addition of LPS had very little effect on NO activity. Nonetheless, these nitrite levels were lower compared to the LPS-activated control group.

It has been shown that macrophage exhibit a foreign body response when they come in contact with an implant [Anderson, 2006]. At the same time, gelatin has been previously identified to as a potential source of endotoxin that could trigger an immune

response [Gorbet et al. 2005]; moreover, the oHA used for this experiment was not tested for its endotoxin content. These factors could be contributory to the increased NO levels of the OG group in its resting state. Conversely, HA has been shown to exert beneficial influence in cases of inflammation and wound healing by suppressing activation of NF-κB, a transcription factor for iNOS expression [Takahashi et al. 2001; Liao, 2005; Yasuda, 2007]. This phenomenon could be a contributing factor of the mild inhibition of NO level in OG activated group.

With the macrophages at their resting state, the media nitrite concentrations in 0.2, 1 and 2% GOG groups were 6.86 ± 1.69, 6.35 ± 0.47, and 5.42 ± 0.41 μM, respectively, after 24 hours. There was no significant difference between these results and the control group at resting state. The data clearly showed a different response of macrophages in OG and 0.2, 1 and 2% GOG groups. The foreign body response observed in the macrophages of the OG group was evidently suppressed in all three GED-containing groups by the released iNOS inhibitor.

The media nitrite contents of 0.2, 1, or 2% GOG groups with LPS pre-activated macrophages were 9.79 ± 4.97, 8.30 ± 1.54, and 6.58 ± 1.36 μM, respectively, after 24 hours. There was a significant difference between these values and the amount of nitrite produced by LPS-stimulated macrophages in the activated control group as well as in the activated OG group ($p<0.05$). Among three GED-containing groups there was no significant difference found between the amount of nitrite produced by macrophages in the resting and LPS-stimulated states. These results confirmed release of GED from microspheres and its efficacy as NO production inhibitor.

It should be noted that proliferation of macrophages over the course of this experiment (24 hours) was not monitored. As was shown previously in section *4.2.1*., GED has an inhibitory effect on macrophage proliferation and viability. Therefore, the number of viable macrophages was likely different in the experimental groups after 24 hours.

The response of iNOS is known to be different in mouse and human cells; after LPS-treatment, iNOS begins expressing in murine macrophages; however, iNOS is almost irresponsive to stimulation in most human macrophages [Schneemann et al. 2007]. Some studies also demonstrate elevated levels of iNOS and NO in adipose tissue of obese patients [Annane et al. 2000; Weisberg et al. 2003]. Therefore, future experiments could be directed towards developing a better understanding of iNOS response in adipose tissue in humans and its inhibition by GED.

4.2.3. Cytokine (IL-1β, TNF-α) release

The amount of cytokines released was determined and the results (average ± S.E.M.) for IL-1β and TNF-α were shown in Figure 10 (A) and 10 (B), respectively. After 24 hours of incubation, IL-1β concentrations of the control groups, in resting state and after LPS stimulation, were 34.89 ± 26.23 pg/ml and 606.49 ± 129.66 pg/ml, respectively. Likewise, the IL-1β concentrations in the OG group, at resting and LPS-activated state, were 78.86 ± 41.69 and 416.17 ± 160.87 pg/ml, respectively. These results suggested a moderate activation of macrophages in the resting state by the hydrogel film and some degrees of inhibition of macrophage in its LPS-stimulated state for the reasons discussed in section *4.2.2*.

Macrophages, in their resting state, in 0.2, 1 and 2% GOG groups released IL-1β, the concentrations were 141.46 ± 22.52, 168.57 ± 47.98 and 159.31 ± 47.33 pg/ml, respectively, which were higher than those produced by macrophages, also in their resting state, in both the control and OG groups. The IL-1β concentrations of the media of LPS-stimulated macrophages were 132.91 ± 76.25, 202.62 ± 51.18 and 166.62 ± 23.96, in the 0.2, 1 and 2% GOG groups, respectively. The amounts of IL-1β released by the LPS-stimulated macrophages in all three GED-containing groups were significantly lower than those of their counterparts in both the activated control group and OG group ($p<0.05$). There was no significant difference in the results of three GED-containing groups between their resting and LPS-activated states.

NO is a known pathway for IL-1 modulation [Hill et al. 1996]. Foreign body response in macrophages could have triggered the expression of the cytokines. Since NO is not the only mediator of IL-1 levels and other cytokines influencing IL-1 expression, it could lead to slightly elevated levels of IL-1β even in the resting state [Dinarello, 1992].

The results revealed that the presence of GED significantly lowered the levels of IL-1β as compared to those of the control groups with macrophages at their activated state; this data was consistent with previous researches [Hill et al. 1996; Aldridge et al. 2008]. IL-1β is one of the pro-inflammatory cytokines, its decrease could result in a partial inhibition of the inflammatory response.

The levels of TNF-α in the control group were, respectively, 316.19 ± 183.63 pg/ml in the resting state and 4992.83 ± 289.82 pg/ml in the LPS-stimulated state. For comparison, TNF-α levels in the OG group were, respectively, 3380.75 ± 276.72 pg/ml in the resting state and 3798.82 ± 244.19 pg/ml in the LPS-stimulated state. The direct

implication was a strong activation of macrophages in the OG group in the resting state, but there was no significant increase in TNF-α level when the macrophages were stimulated with LPS. As alluded to previously, activation of macrophages in the resting state was most likely caused by the foreign body response leading to elevated TNF-α levels. Concurrently, this increase could be due to a potential presence of endotoxins in the microsphere system. As described in section *4.2.2.*, HA has the capacity of inhibiting activation of NF-κB, a transcription factor for cytokines expression thus, modulating TNF-α expression during LPS stimulation [Yasuda, 2007].

TNF-α levels in 0.2% GOG, 1% GOG and 2% GOG were, respectively, 4151.63 ± 693.89, 2977.12 ± 214.81 and 4529.71 ± 412.01 pg/ml for macrophages in their resting state; and, 5194.48 ± 268.69, 4289.17 ± 519.89, and 4808.89 ± 90.85 pg/ml, respectively, after 24 hours of LPS stimulation. Only the macrophages in 1% GOG group released the amount of TNF-α that was significantly different from that of the LPS-treated control group ($p<0.05$), this result suggested that GED concentration could be adjusted to produce a stronger effect on TNF-α release.

The pathways for mediation of TNF-α are similar but not exclusive to the activation pathways of IL-1β. LPS triggers the activation of NF-κB, leading to the expression of TNF-α, IL-1β, other cytokines and iNOS [Winston et al. 1999]. TNF-α induces expression of more pro-inflammatory cytokines including a positive feedback on itself, which could be controlled by anti-inflammatory cytokines [Winston et al. 1999; Schwentker et al. 2002]. Previous work showed that NO-releasing agents could influence expression of TNF-α depending on stimulation pathway; LPS-induced TNF-α levels decreased with elevation in NO concentration produced by NO-releasing agents [Eigler et

al. 1993]. Our results showed that the response of TNF-α to the presence of an iNOS inhibitor was not dose-dependant. The effect of GED on TNF-α production should be investigated further in order to determine the underlying interactive mechanism of TNF-α and GED in order to facilitate further optimization of the GED concentrations in microspheres formulations.

As alluded to previously in section *4.2.2.*, the growth of macrophages was most likely altered by GED over the course of 24 hour. Future study on the amount of released NO and cytokines should be normalized by the cell number.

Figure 7. Macrophage proliferation and morphology.
50,000 cells per group were seeded initially. Control group: day 3 (A), day 14 (B); OG group: day 3 (C), day 14 (D); 0.2% GOG: day 3 (E), day 14 (F); 1% GOG: day 3 (G), day 14 (H); 2% GOG: day 3 (I), day 14 (J).

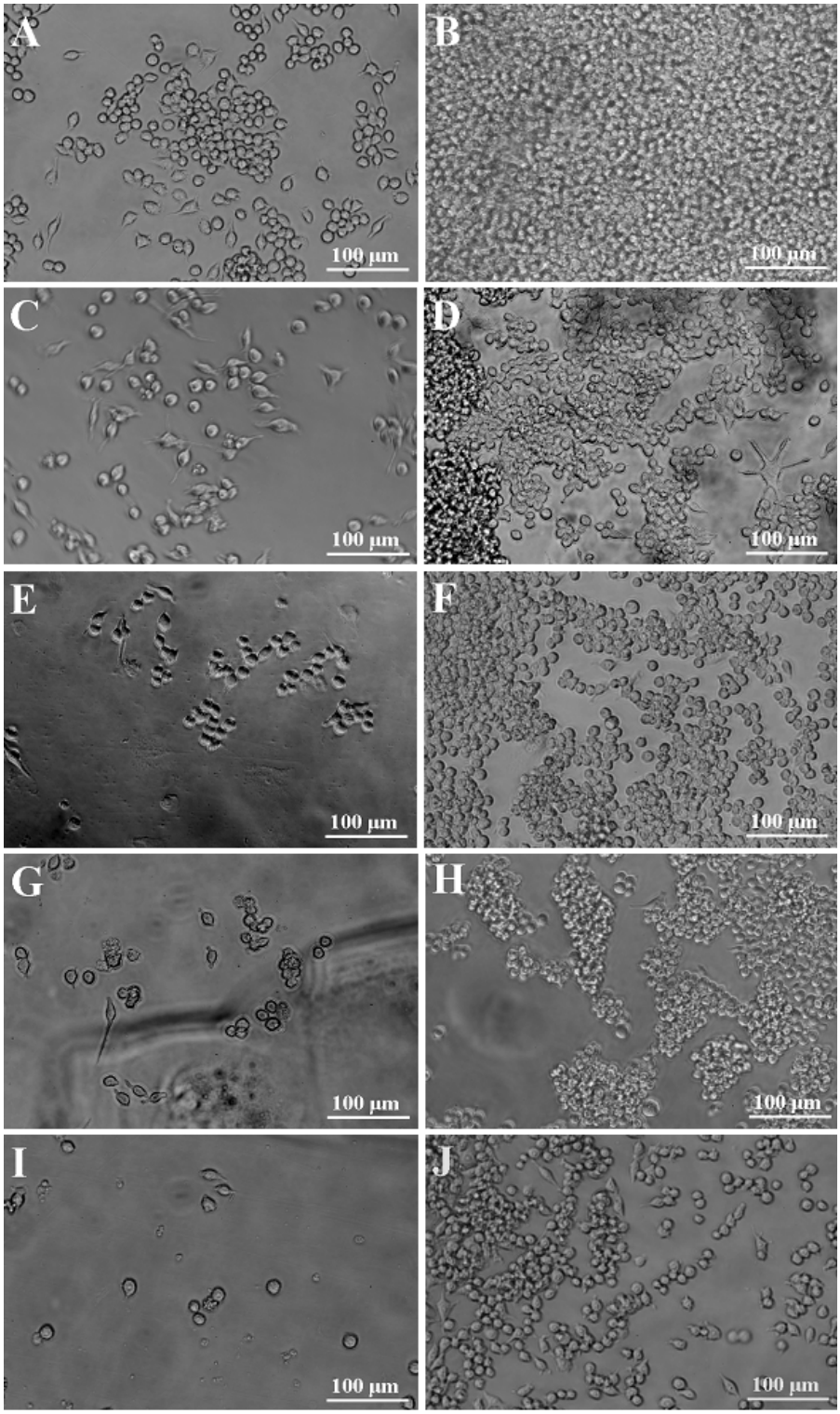

Figure 8. Macrophage density (A) and viability (B).
50,000 cells per group were seeded without any hydrogel (control), in OG group, and in 0.2, 1 and 2 % GOG groups.
(*) indicates a significant difference from LPS-treated control group and from LPS-treated OG group ($p<0.05$);
(**) indicates a significant difference from LPS-treated control group ($p<0.05$)

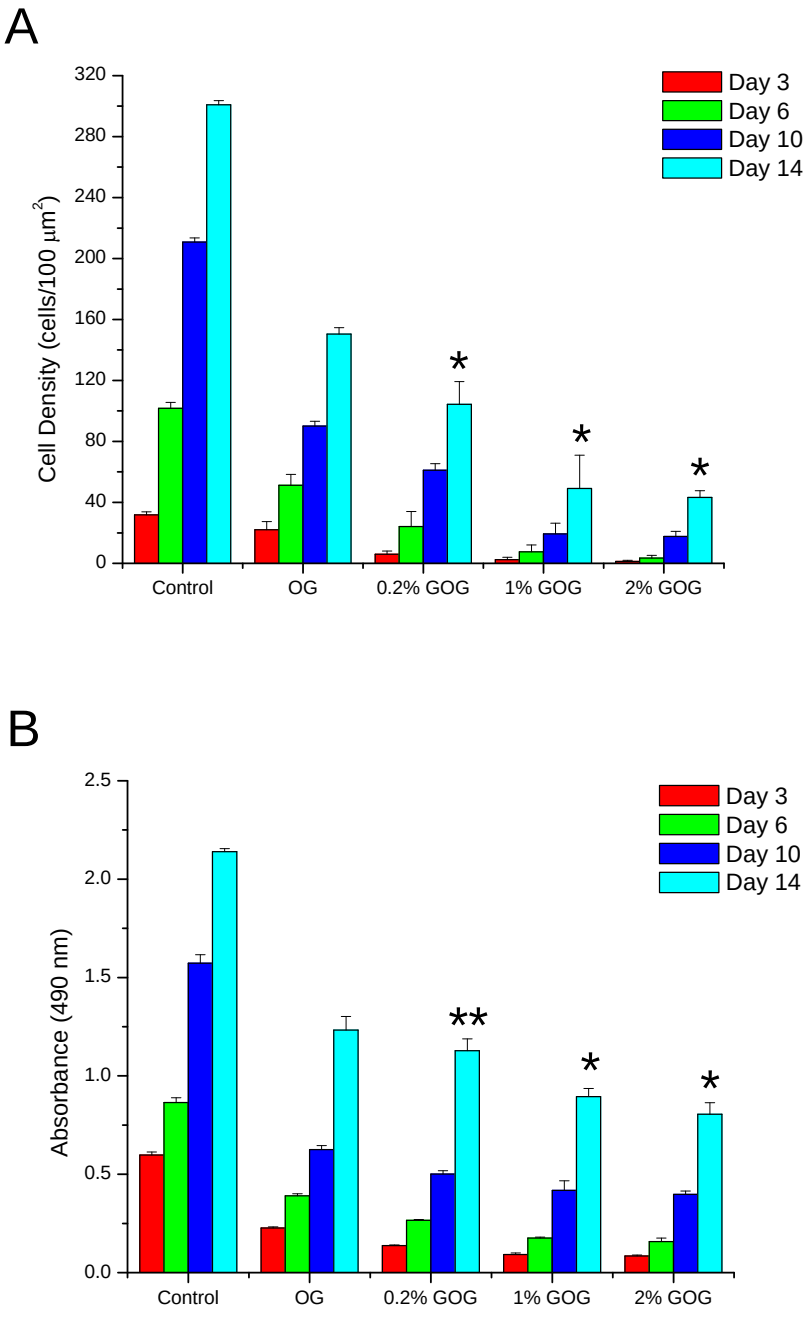

Figure 9. NO release from macrophages.
500,000 cells per group were seeded without any hydrogel (control), in OG group, and in 0.2, 1 and 2 % GOG groups.
(*) indicates a significant difference from LPS-treated control group and a significant difference from LPS-treated OG group ($p<0.05$).

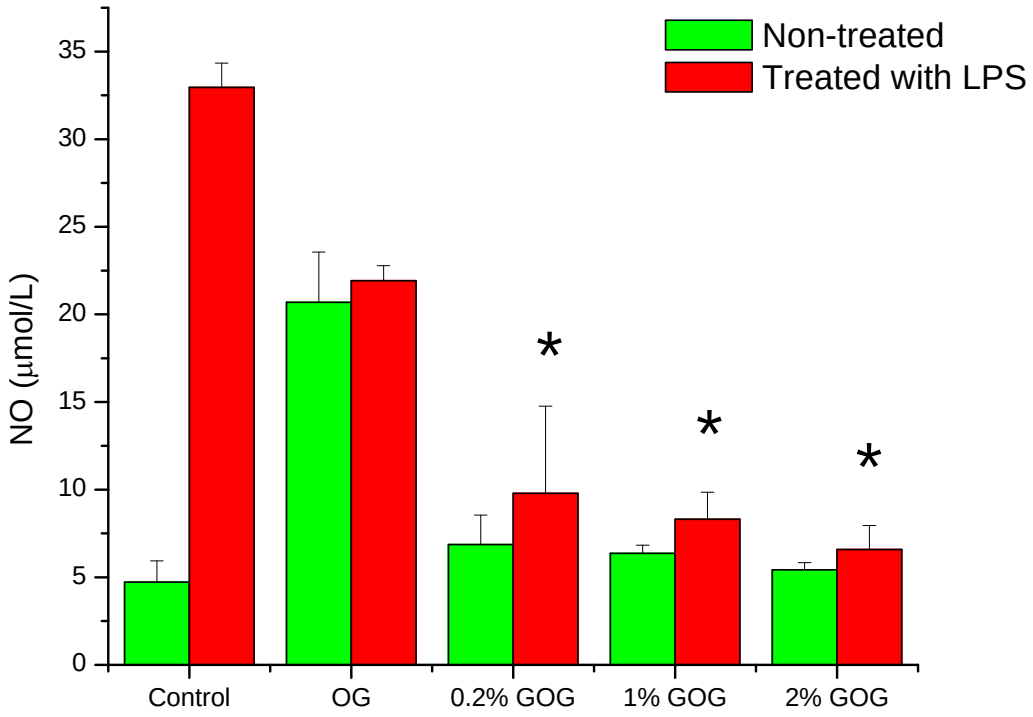

Figure 10. IL-1 β (A) and TNF-α (B) release from macrophages.
500,000 cells per group were seeded without any hydrogel (control), in OG group, and in 0.2, 1 and 2 % GOG groups.
***) indicates a significant difference from LPS-treated control group and from LPS-treated OG group ($p<0.05$);**
(**) indicates a significant difference from LPS-treated control group ($p<0.05$).

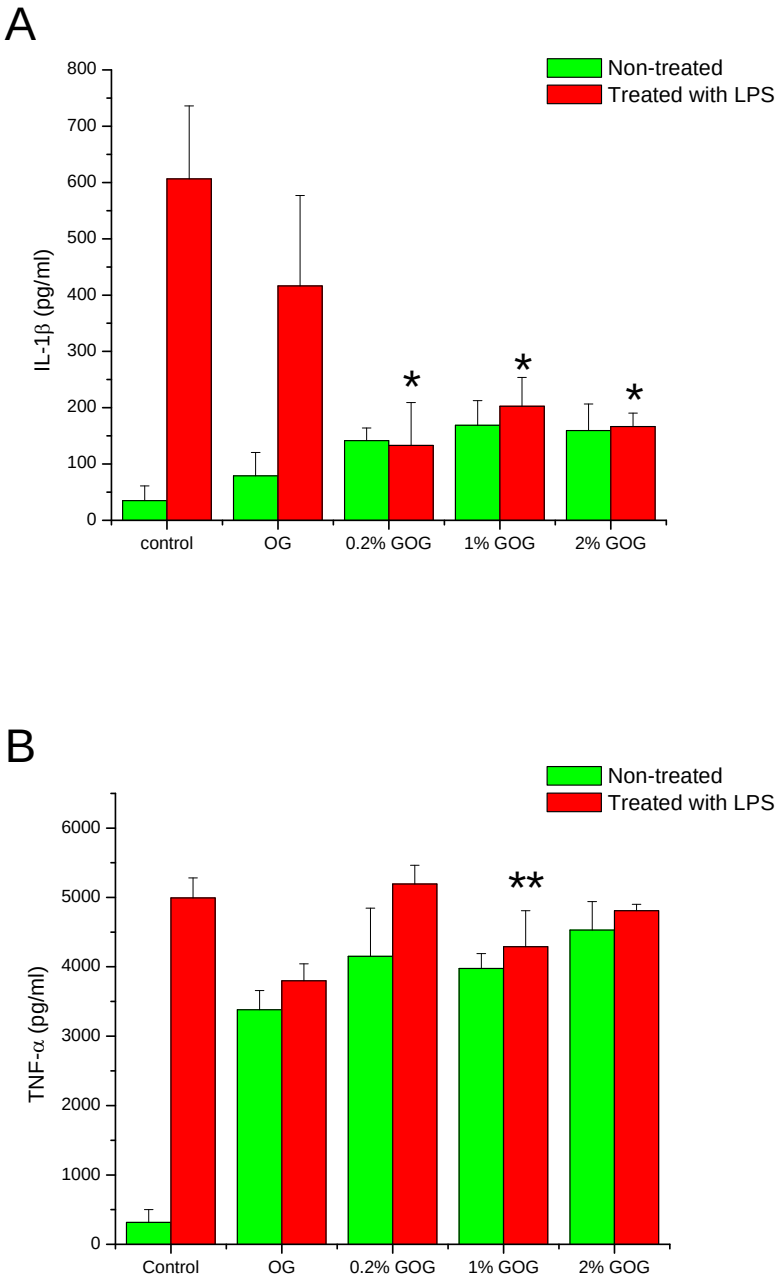

CHAPTER 5

BIOCOMPATIBILITY AND POTENTIAL ANTI-INFLAMMATORY EFFECT OF GED-LOADED MICROSPHERES *IN VIVO*

Specific aim 3: Evaluation of biocompatibility and efficacy *in vivo* of crosslinker-free microsphere system with incorporated iNOS inhibitor.

Experiments and analyses described in this chapter were done in collaboration with Dr. Weiliam Chen, the Principal Investigator of this project, Dr. Julia Zakhaleva, and Dr. Lihui Weng, a former Post-doctoral Fellow in Weiliam Chen's lab. Dr. Chen, Dr. Zakhaleva and Dr. Weng participated in animal surgeries and histology slide analyses. Natalia Ivanova participated in histology slide analyses and contributed to approximately one-fifth of the work. The results presented in this chapter were published: L. Weng, N. D. Ivanova, J. Zakhaleva, W. Chen. *In vitro* and *in vivo* suppression of cellular activity by guanidinoethyl disulfide released from hydrogel microspheres composed of partially oxidized hyaluronan and gelatin. *Biomaterials* **29**, 4149 (Nov, 2008).

5.1 Materials and Methods

The efficacy of released GED from oHA/Gelatin microspheres *in vivo* was studied using a mouse transcutaneous implant model. All animals were treated according to the protocol approved by SUNY-Stony Brook IACUC. Adult male mice (5 weeks old, Balb/cJ strain, Jackson Lab, Bar Harbor, ME) were anesthetized with isoflurane (5% for

induction and 2.5% for maintenance). Round incisional wound was made in dorsal midline skin with a biopsy needle (diameter: 8mm, Miltex, Japan). The implants were round hydrogel films (diameter: 8 mm, thickness: 0.5 mm) with 1% GED-loaded microspheres (1% GOG) and plain films (OG) were used as control. The films were prepared as described in section *4.1.2.*, Chapter 4. All implants were sterilized with 70% ethanol and rehydrated with sterile saline. Hydrogel film was implanted into the fresh wound, plastered with Tegaderm™ and overlaid with a Band-Aid. A dose of buprenorphine (0.05 to 0.1 mg/kg, sub-Q) was administered after the procedure for pain control.

Animals were euthanized at days 3 and 7. Implanted hydrogels with surrounding tissue were excised, fixed with 10% neutral buffered formalin, processed, paraffin embedded, and stained with hematoxylin and eosin (H&E).

5.2 Results and Discussion

Figure 11 showed a typical incisional wound with implanted hydrogel and covered with Tegaderm™. Animals tolerated the operation well and didn't show any adverse reaction to the implants during the course of experiment.

During wound healing, the prominent cell types present at the wound site to interact with implanted materials are macrophages and fibroblasts; these two cell types also modulate the functions of each other [Clark, 1996]. Activation of macrophages in the wound area occurs almost immediately; their abundance reaches the maximum by day 3 and starts to decline by day 6-7. Therefore, days 3 and 7 were chosen for observation of GED's effect on cell proliferation and wound healing.

Histological results of day 3 and day 7 were presented in Figure 12. Figure 12 (A) and (B) revealed the progression of cellular infiltration and healing in a wound bed without the implant. Analyses of the OG group (no GED) depicted cells infiltrated deeply (~75%) into the hydrogel implant by day 3 (Figure 12 (C)), with extensive infiltration of cells occurred by day 7 (Figure 12 (D)). In contrast, at day 3, the histological section of the wound bed implanted with the GOG hydrogel group (Figure 12 (E)) showed very little cell infiltration into the gel indicating inhibitory effect of GED. By day 7 (Figure 12 (F)), cells infiltrated approximately half-way into the hydrogel. Ten random microscopic fields were selected for both hydrogel systems and the numbers of cells were counted manually. The ratios of infiltrated cells in OG and 1% GOG groups were 4.8:1 by day 3 and 6.2:1 by day 7, signifying sustained release of GED from the microspheres.

There was a clear difference between the hydrogels' thicknesses and staining intensities between the OG and GOG groups. By day 3, the OG hydrogel appeared swollen and become less distinguishable from the surrounding tissue. Both HA and gelatin are susceptible to enzymatic degradation, partial digestion of the hydrogel resulted in destruction of the crosslinking bonds, decrease its resistance to water-uptake, and caused swelling of the implant. Hydrogel degradation/swelling was a direct result of cellular infiltration and also signifying the beginning of tissue regeneration. Conversely, the histological sections of the wound bed implanted with 1% GOG group (Figure 12 (E, F)) demonstrated a very distinct line between the GED-containing implant and surrounding tissue at both time points, little swelling and stronger staining intensity than

that of the OG group. Continuous suppression of cellular infiltration and activity by GED lead to preservation of implant integrity.

Figure 11. The digital image of the wound bed in the transcutaneous experiment.

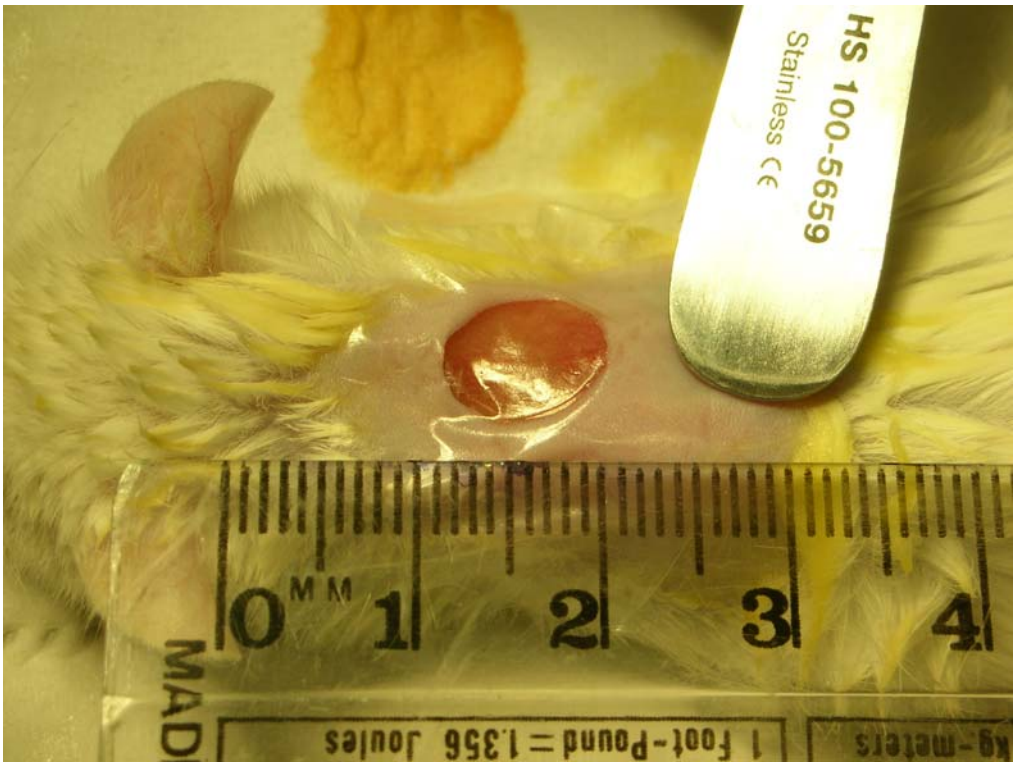

Figure 12[7]. H&E staining for the implants explanted after 3 days: Control (A), OG (C), 1% GOG (E); 7 days: Control (B), OG (D), 1% GOG (F). I: Implant; L: Loose connective tissue; ↑: Cells. Images were captured under 20 × magnification.

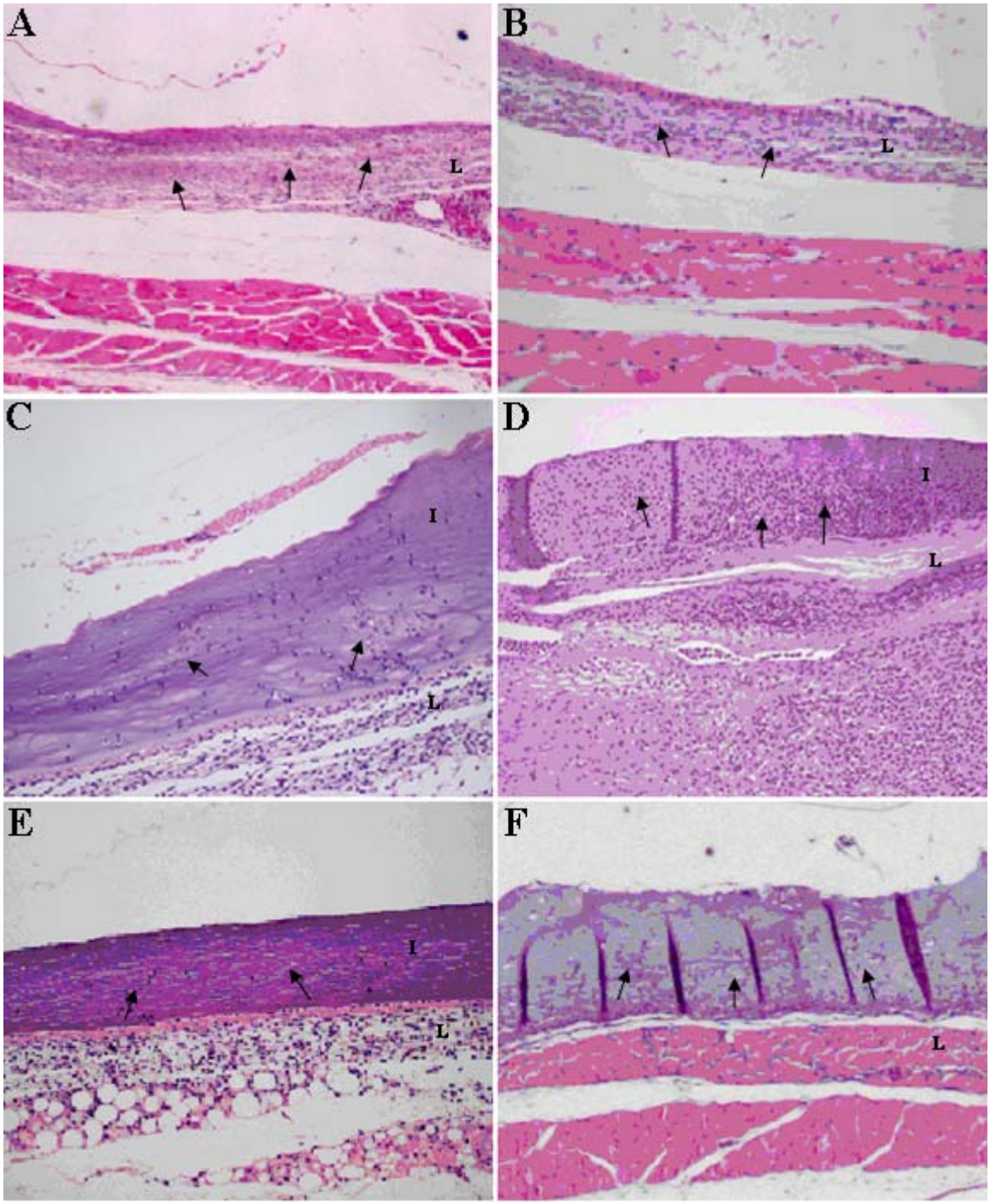

[7] Modified image was adopted from Weng et al. 2008(b).

CHAPTER 6

CONCLUSION

We have formulated self-crosslinking microspheres composed of oxidized hyaluronan (oHA) and gelatin. This system was designed as a drug delivery carrier for an iNOS inhibitor, guanidinoethy disulfide (GED).

Microspheres formulated from a crosslinker-free process could greatly reduce the cytotoxicity potential upon degradation. The drug release profiles confirmed a successful entrapment and release of GED. Analyses of particle morphology revealed a porous structure of fully-swollen microspheres, which was an important feature for drug diffusion and release. Further investigations showed continuous release of GED for at least one week with after the initial burst release. Therefore, this microsphere system could be formulated to prolong GED's efficacy. The study also showed a strong inverse correlation between the GED content and the microsphere size as well as the swelling ratio. Thus, the physical parameters of the microsphere system could be modulated to achieve the desired properties depending on application.

The effect of the microsphere system *in vitro* was investigated using a macrophage model. Macrophages were chosen since they are one of the most important cells during wound healing and their activities modulate the course of inflammation and transition to re-epithelization/remodeling stages. Our results showed that the GED content had an inverse effect on cellular proliferation, density and viability over the course of two weeks. However, daily media change could have altered the analyses by removal of dead cells; future studies should further investigate the effect of GED on

apoptosis. Hitherto, our experiments were preformed using cell lines which differ considerably from primary cells; future studies will focus on the effect of GED on primary cells.

Analyses of GED's effect *in vitro* also included observations of NO and cytokine (TNF-α and IL-1β) release over 24 hours. We found a sustained inhibition of NO and IL-1β in LPS-activated macrophages with GED-loaded microspheres. Suppression of NO confirmed the *in vitro* efficacy GED, a known iNOS inhibitor. NO, a physiological messenger molecule, was also found to mediate release of pro-inflammatory cytokine IL-1β confirming previous research [Hill et al. 1996]. Further studies should also be conducted to evaluate the expression of both iNOS and NO levels in human adipose tissue and their response to GED treatment.

The release of TNF-α was found to be less affected by the presence of GED. In fact, only the 1% GED-loaded microspheres were able to significantly suppress TNF-α compared to the control group. There were several possibilities of the phenomenon observed. The results of previous studies showed that mediation of TNF-α by NO was dependent on activation pathway; it was noted that TNF-α activated by LPS decreased during application of NO-releasing agents [Eigel et al. 1993]. iNOS expression does not start immediately after LPS-stimulation; there could have been an accumulation of strong TNF-α expression during that lag phase. Further studies are needed to fully elucidate the relationships between GED application and expression of TNF-α.

Both the biocompatibility and efficacy of GED-loaded microspheres were evaluated *in vivo* using mouse transcutaneous dermal wound model. Days 3 and 7 were chosen for observation of the wound site and the implants. The results revealed the

suppression of cellular infiltration in the presence of GED-loaded microspheres by day 3 and the effect persisted at day 7. Histology images showed a decrease in the number of cells surrounding the implant, suggesting an inhibition of inflammation. Future dose-response studies should be completed and tested using a disease model.

BIBLIOGRAPHY

[1] A.H.L. Abul K. Abbas, Shiv Pillai, Cellular and molecular immunology, Saunders Elsevier, Philadelphia, 2007.
[2] C. Aldridge, A. Razzak, T.A. Babcock, W.S. Helton, N.J. Espat, Lipopolysaccharide-stimulated RAW 264.7 macrophage inducible nitric oxide synthase and nitric oxide production is decreased by an omega-3 fatty acid lipid emulsion. The Journal of surgical research 149(2) (2008) 296-302.
[3] K. Alexandraki, C. Piperi, C. Kalofoutis, J. Singh, A. Alaveras, A. Kalofoutis, Inflammatory process in type 2 diabetes: The role of cytokines. Annals of the New York Academy of Sciences 1084 (2006) 89-117.
[4] J.A. Anderson, in: J. D. Bronzino (Ed.), The biomedical engineering handbook, CRC, 2006, pp. 5-7.
[5] J.M. Anderson, A. Rodriguez, D.T. Chang, Foreign body reaction to biomaterials. Seminars in immunology 20(2) (2008) 86-100.
[6] D. Annane, S. Sanquer, V. Sebille, A. Faye, D. Djuranovic, J.C. Raphael, P. Gajdos, E. Bellissant, Compartmentalised inducible nitric-oxide synthase activity in septic shock. Lancet 355(9210) (2000) 1143-1148.
[7] M. Arnush, M.R. Heitmeier, A.L. Scarim, M.H. Marino, P.T. Manning, J.A. Corbett, IL-1 produced and released endogenously within human islets inhibits beta cell function. The Journal of clinical investigation 102(3) (1998) 516-526.
[8] V. Arzumanian, E. Stankevicius, A. Laukeviciene, E. Kevelaitis, [Mechanisms of nitric oxide synthesis and action in cells]. Medicina (Kaunas, Lithuania) 39(6) (2003) 535-541.
[9] C.E.L. Bernard Burke, The Macrophage, Oxford, 2002.
[10] S. Bird, J. Zou, T. Wang, B. Munday, C. Cunningham, C.J. Secombes, Evolution of interleukin-1beta. Cytokine & growth factor reviews 13(6) (2002) 483-502.
[11] R. Blakytny, E. Jude, The molecular biology of chronic wounds and delayed healing in diabetes. Diabet Med 23(6) (2006) 594-608.
[12] J.S. Boateng, K.H. Matthews, H.N. Stevens, G.M. Eccleston, Wound healing dressings and drug delivery systems: a review. Journal of pharmaceutical sciences 97(8) (2008) 2892-2923.
[13] L. Bosca, M. Zeini, P.G. Traves, S. Hortelano, Nitric oxide and cell viability in inflammatory cells: a role for NO in macrophage function and fate. Toxicology 208(2) (2005) 249-258.
[14] H. Brem, M. Tomic-Canic, Cellular and molecular basis of wound healing in diabetes. The Journal of clinical investigation 117(5) (2007) 1219-1222.
[15] M.B. Brown, S.A. Jones, Hyaluronic acid: a unique topical vehicle for the localized delivery of drugs to the skin. J Eur Acad Dermatol Venereol 19(3) (2005) 308-318.
[16] O. Cantoni, L. Palomba, A. Guidarelli, I. Tommasini, L. Cerioni, P. Sestili, Cell signaling and cytotoxicity by peroxynitrite. Environmental health perspectives 110 Suppl 5 (2002) 823-825.
[17] F.M. Chen, Y.M. Zhao, H. Wu, Z.H. Deng, Q.T. Wang, W. Zhou, Q. Liu, G.Y. Dong, K. Li, Z.F. Wu, Y. Jin, Enhancement of periodontal tissue regeneration by locally

controlled delivery of insulin-like growth factor-I from dextran-co-gelatin microspheres. J Control Release 114(2) (2006) 209-222.
[18] R.A. Clark, Fibrin and wound healing. Annals of the New York Academy of Sciences 936 (2001) 355-367.
[19] R.A. Clark, Fibrin is a many splendored thing. The Journal of investigative dermatology 121(5) (2003) xxi-xxii.
[20] R.A.F. Clark, The molecular and cellular biology of wound repair, Plenum Press, New York, 1996.
[21] C.J. Coester, K. Langer, H. van Briesen, J. Kreuter, Gelatin nanoparticles by two step desolvation--a new preparation method, surface modifications and cell uptake. Journal of microencapsulation 17(2) (2000) 187-193.
[22] J.W. Coleman, Nitric oxide in immunity and inflammation. International immunopharmacology 1(8) (2001) 1397-1406.
[23] R. Cortesi, E. Esposito, M. Osti, G. Squarzoni, E. Menegatti, S.S. Davis, C. Nastruzzi, Dextran cross-linked gelatin microspheres as a drug delivery system. Eur J Pharm Biopharm 47(2) (1999) 153-160.
[24] A.M. Deakin, A.N. Payne, B.J. Whittle, S. Moncada, The modulation of IL-6 and TNF-alpha release by nitric oxide following stimulation of J774 cells with LPS and IFN-gamma. Cytokine 7(5) (1995) 408-416.
[25] C.A. Dinarello, The biology of interleukin-1. Chemical immunology 51 (1992) 1-32.
[26] C.A. Dinarello, Interleukin-1. Cytokine & growth factor reviews 8(4) (1997) 253-265.
[27] A. Eigler, J. Moeller, S. Endres, Exogenous and endogenous nitric oxide attenuates tumor necrosis factor synthesis in the murine macrophage cell line RAW 264.7. J Immunol 154(8) (1995) 4048-4054.
[28] A. Eigler, B. Sinha, S. Endres, Nitric oxide-releasing agents enhance cytokine-induced tumor necrosis factor synthesis in human mononuclear cells. Biochemical and biophysical research communications 196(1) (1993) 494-501.
[29] E. Esposito, E. Menegatti, R. Cortesi, Hyaluronan-based microspheres as tools for drug delivery: a comparative study. International journal of pharmaceutics 288(1) (2005) 35-49.
[30] K.S. Farley, L.F. Wang, C. Law, S. Mehta, Alveolar macrophage inducible nitric oxide synthase-dependent pulmonary microvascular endothelial cell septic barrier dysfunction. Microvascular research 76(3) (2008) 208-216.
[31] N. Fujiwara, K. Kobayashi, Macrophages in inflammation. Current drug targets 4(3) (2005) 281-286.
[33] D.A. Geller, T.R. Billiar, Molecular biology of nitric oxide synthases. Cancer metastasis reviews 17(1) (1998) 7-23.
[33] M.B. Gorbet, M.V. Sefton, Endotoxin: the uninvited guest. Biomaterials 26(34) (2005) 6811-6817.
[34] A.K. Gupta, M. Gupta, S.J. Yarwood, A.S. Curtis, Effect of cellular uptake of gelatin nanoparticles on adhesion, morphology and cytoskeleton organisation of human fibroblasts. J Control Release 95(2) (2004) 197-207.
[35] D.J. Hackam, H.R. Ford, Cellular, biochemical, and clinical aspects of wound healing. Surgical infections 3 Suppl 1 (2002) S23-35.

[36] K.G. Harding, H.L. Morris, G.K. Patel, Science, medicine and the future: healing chronic wounds. BMJ (Clinical research ed 324(7330) (2002) 160-163.
[37] M.R. Heitmeier, A.L. Scarim, J.A. Corbett, Interferon-gamma increases the sensitivity of islets of Langerhans for inducible nitric-oxide synthase expression induced by interleukin 1. The Journal of biological chemistry 272(21) (1997) 13697-13704.
[38] J.R. Hill, J.A. Corbett, G. Kwon, C.A. Marshall, M.L. McDaniel, Nitric oxide regulates interleukin 1 bioactivity released from murine macrophages. The Journal of biological chemistry 271(37) (1996) 22672-22678.
[39] H.E. Hohmeier, V.V. Tran, G. Chen, R. Gasa, C.B. Newgard, Inflammatory mechanisms in diabetes: lessons from the beta-cell. Int J Obes Relat Metab Disord 27 Suppl 3 (2003) S12-16.
[40] M. Holstad, L. Jansson, S. Sandler, Inhibition of nitric oxide formation by aminoguanidine: an attempt to prevent insulin-dependent diabetes mellitus. General pharmacology 29(5) (1997) 697-700.
[41] W. Hornebeck, Down-regulation of tissue inhibitor of matrix metalloprotease-1 (TIMP-1) in aged human skin contributes to matrix degradation and impaired cell growth and survival. Pathologie-biologie 51(10) (2003) 569-573.
[42] S.T. Huang, C.S. Ho, C.M. Lin, H.W. Fang, Y.X. Peng, Development and biological evaluation of C(60) fulleropyrrolidine-thalidomide dyad as a new anti-inflammation agent. Bioorganic & medicinal chemistry 16(18) (2008) 8619-8626.
[43] B.J. Jia XQ, Kobler J, Clifton RJ, Rosowski JJ, Zeitels SM et al., Synthesis and characterization of in situ cross-linkable hyaluronic acid-based hydrogels with potential application for vocal cord regeneration. Macromolecules 37 (2004) 3239-3248.
[44] J.S. Kang, Y.J. Jeon, H.M. Kim, S.H. Han, K.H. Yang, Inhibition of inducible nitric-oxide synthase expression by silymarin in lipopolysaccharide-stimulated macrophages. The Journal of pharmacology and experimental therapeutics 302(1) (2002) 138-144.
[45] J.A. Knight, Review: Free radicals, antioxidants, and the immune system. Annals of clinical and laboratory science 30(2) (2000) 145-158.
[46] C.B. Knudson, W. Knudson, Cartilage proteoglycans. Seminars in cell & developmental biology 12(2) (2001) 69-78.
[47] M.N. Kumar, N. Kumar, Polymeric controlled drug-delivery systems: perspective issues and opportunities. Drug development and industrial pharmacy 27(1) (2001) 1-30.
[48] D.A. Ledward, in: P. A. W. G. O. Phillips (Ed.), Handbook of Hydrocolloids, CRC, 2000, pp. 67-86.
[49] R.H. Lee, D. Efron, U. Tantry, A. Barbul, Nitric oxide in the healing wound: a time-course study. The Journal of surgical research 101(1) (2001) 104-108.
[50] G. Lemperle, V.B. Morhenn, V. Pestonjamasp, R.L. Gallo, Migration studies and histology of injectable microspheres of different sizes in mice. Plastic and reconstructive surgery 113(5) (2004) 1380-1390.
[51] H.C. Liang, W.H. Chang, K.J. Lin, H.W. Sung, Genipin-crosslinked gelatin microspheres as a drug carrier for intramuscular administration: in vitro and in vivo studies. Journal of biomedical materials research 65(2) (2003) 271-282.
[52] Y.H. Liao, S.A. Jones, B. Forbes, G.P. Martin, M.B. Brown, Hyaluronan: pharmaceutical characterization and drug delivery. Drug delivery 12(6) (2005) 327-342.

[53] S.T. Lim, B. Forbes, G.P. Martin, M.B. Brown, In vivo and in vitro characterization of novel microparticulates based on hyaluronan and chitosan hydroglutamate. AAPS PharmSciTech 2(4) (2001) 20.
[54] J.G. Mabley, G.J. Southan, A.L. Salzman, C. Szabo, The combined inducible nitric oxide synthase inhibitor and free radical scavenger guanidinoethyldisulfide prevents multiple low-dose streptozotocin-induced diabetes in vivo and interleukin-1beta-induced suppression of islet insulin secretion in vitro. Pancreas 28(2) (2004) E39-44.
[55] J. Marcinkiewicz, A. Grabowska, B. Chain, Nitric oxide up-regulates the release of inflammatory mediators by mouse macrophages. European journal of immunology 25(4) (1995) 947-951.
[56] K. Maruyama, J. Asai, M. Ii, T. Thorne, D.W. Losordo, P.A. D'Amore, Decreased macrophage number and activation lead to reduced lymphatic vessel formation and contribute to impaired diabetic wound healing. The American journal of pathology 170(4) (2007) 1178-1191.
[57] C. Napoli, F. de Nigris, W. Palinski, Multiple role of reactive oxygen species in the arterial wall. Journal of cellular biochemistry 82(4) (2001) 674-682.
[58] A. Neumann, R. Schinzel, D. Palm, P. Riederer, G. Munch, High molecular weight hyaluronic acid inhibits advanced glycation endproduct-induced NF-kappaB activation and cytokine expression. FEBS letters 453(3) (1999) 283-287.
[59] N.J. Percival, Classification of wounds and their management. Surgery (Oxford) 20(5) (2002) 114-117.
[60] D. Sarkar, P. Saha, S. Gamre, S. Bhattacharjee, C. Hariharan, S. Ganguly, R. Sen, G. Mandal, S. Chattopadhyay, S. Majumdar, M. Chatterjee, Anti-inflammatory effect of allylpyrocatechol in LPS-induced macrophages is mediated by suppression of iNOS and COX-2 via the NF-kappaB pathway. International immunopharmacology 8(9) (2008) 1264-1271.
[61] M. Schneemann, G. Schoeden, Macrophage biology and immunology: man is not a mouse. Journal of leukocyte biology 81(3) (2007) 579; discussion 580.
[62] M.M. Schroeder, R.J. Belloto, Jr., R.A. Hudson, M.F. McInerney, Effects of antioxidants coenzyme Q10 and lipoic acid on interleukin-1 beta-mediated inhibition of glucose-stimulated insulin release from cultured mouse pancreatic islets. Immunopharmacology and immunotoxicology 27(1) (2005) 109-122.
[63] A. Schwentker, Y. Vodovotz, R. Weller, T.R. Billiar, Nitric oxide and wound repair: role of cytokines? Nitric Oxide 7(1) (2002) 1-10.
[64] T. Segura, B.C. Anderson, P.H. Chung, R.E. Webber, K.R. Shull, L.D. Shea, Crosslinked hyaluronic acid hydrogels: a strategy to functionalize and pattern. Biomaterials 26(4) (2005) 359-371.
[65] E.M. Shin, H.Y. Zhou, L.Y. Guo, J.A. Kim, S.H. Lee, I. Merfort, S.S. Kang, H.S. Kim, S. Kim, Y.S. Kim, Anti-inflammatory effects of glycyrol isolated from Glycyrrhiza uralensis in LPS-stimulated RAW264.7 macrophages. International immunopharmacology 8(11) (2008) 1524-1532.
[66] X.Z. Shu, Y. Liu, F. Palumbo, G.D. Prestwich, Disulfide-crosslinked hyaluronan-gelatin hydrogel films: a covalent mimic of the extracellular matrix for in vitro cell growth. Biomaterials 24(21) (2003) 3825-3834.
[67] W.L. Suarez-Pinzon, J.G. Mabley, K. Strynadka, R.F. Power, C. Szabo, A. Rabinovitch, An inhibitor of inducible nitric oxide synthase and scavenger of

peroxynitrite prevents diabetes development in NOD mice. Journal of autoimmunity 16(4) (2001) 449-455.
[68] E. Suzuki, C. Sugiyama, K. Umezawa, Inhibition of inflammatory mediator secretion by (-)-DHMEQ in mouse bone marrow-derived macrophages. Biomedicine & pharmacotherapy = Biomedecine & pharmacotherapie (2008).
[69] C. Szabo, G. Ferrer-Sueta, B. Zingarelli, G.J. Southan, A.L. Salzman, R. Radi, Mercaptoethylguanidine and guanidine inhibitors of nitric-oxide synthase react with peroxynitrite and protect against peroxynitrite-induced oxidative damage. The Journal of biological chemistry 272(14) (1997) 9030-9036.
[70] K. Takahashi, S. Hashimoto, T. Kubo, Y. Hirasawa, M. Lotz, D. Amiel, Hyaluronan suppressed nitric oxide production in the meniscus and synovium of rabbit osteoarthritis model. J Orthop Res 19(3) (2001) 500-503.
[71] M.I. Tammi, A.J. Day, E.A. Turley, Hyaluronan and homeostasis: a balancing act. The Journal of biological chemistry 277(7) (2002) 4581-4584.
[72] H.E. Thomas, R. Darwiche, J.A. Corbett, T.W. Kay, Interleukin-1 plus gamma-interferon-induced pancreatic beta-cell dysfunction is mediated by beta-cell nitric oxide production. Diabetes 51(2) (2002) 311-316.
[73] G. Vallette, A. Jarry, J.E. Branka, C.L. Laboisse, A redox-based mechanism for induction of interleukin-1 production by nitric oxide in a human colonic epithelial cell line (HT29-Cl.16E). The Biochemical journal 313 (Pt 1) (1996) 35-38.
[74] M.A. Vandelli, M. Romagnoli, A. Monti, M. Gozzi, P. Guerra, F. Rivasi, F. Forni, Microwave-treated gelatin microspheres as drug delivery system. J Control Release 96(1) (2004) 67-84.
[75] K.P. Vercruysse, G.D. Prestwich, Hyaluronate derivatives in drug delivery. Critical reviews in therapeutic drug carrier systems 15(5) (1998) 513-555.
[76] Q. Wang, M. Xia, C. Liu, H. Guo, Q. Ye, Y. Hu, Y. Zhang, M. Hou, H. Zhu, J. Ma, W. Ling, Cyanidin-3-O-beta-glucoside inhibits iNOS and COX-2 expression by inducing liver X receptor alpha activation in THP-1 macrophages. Life sciences 83(5-6) (2008) 176-184.
[77] H.J. Wei, H.H. Yang, C.H. Chen, W.W. Lin, S.C. Chen, P.H. Lai, Y. Chang, H.W. Sung, Gelatin microspheres encapsulated with a nonpeptide angiogenic agent, ginsenoside Rg1, for intramyocardial injection in a rat model with infarcted myocardium. J Control Release 120(1-2) (2007) 27-34.
[78] S.P. Weisberg, D. McCann, M. Desai, M. Rosenbaum, R.L. Leibel, A.W. Ferrante, Jr., Obesity is associated with macrophage accumulation in adipose tissue. The Journal of clinical investigation 112(12) (2003) 1796-1808.
[79] K.E. Wellen, Hotamishigil, Gokhal S., Obesity-induced inflammatory changes in adipose tissue. Journal of Clinical Investigation 112(12) (Dec 2003) 1785-1788.
[80](a) L. Weng, H. Pan, W. Chen, Self-crosslinkable hydrogels composed of partially oxidized hyaluronan and gelatin: in vitro and in vivo responses. Journal of biomedical materials research 85(2) (2008) 352-365.
[81](b) L. Weng, N.D. Ivanova, J. Zakhaleva, W. Chen, In vitro and in vivo suppression of cellular activity by guanidinoethyl disulfide released from hydrogel microspheres composed of partially oxidized hyaluronan and gelatin. Biomaterials 29(31) (2008) 4149-4156.

[82] B.W. Winston, P.M. Krein, C. Mowat, Y. Huang, Cytokine-induced macrophage differentiation: a tale of 2 genes. Clinical and investigative medicine 22(6) (1999) 236-255.
[83] T. Yasuda, Hyaluronan inhibits cytokine production by lipopolysaccharide-stimulated U937 macrophages through down-regulation of NF-kappaB via ICAM-1. Inflamm Res 56(6) (2007) 246-253.
[84] Y.H. Yun, D.J. Goetz, P. Yellen, W. Chen, Hyaluronan microspheres for sustained gene delivery and site-specific targeting. Biomaterials 25(1) (2004) 147-157.
[85] M. Zeyda, T.M. Stulnig, Adipose tissue macrophages. Immunology letters 112(2) (2007) 61-67.
[86] S.N. Zykova, T.G. Jenssen, M. Berdal, R. Olsen, R. Myklebust, R. Seljelid, Altered cytokine and nitric oxide secretion in vitro by macrophages from diabetic type II-like db/db mice. Diabetes 49(9) (2000) 1451-1458.